Composites Part C: Open Access 4 (2021) 100113

Contents lists available at ScienceDirect

Composites Part C: Open Access

journal homepage: www.elsevier.com/locate/jcomc

The use of cellulose in bio-derived formulations for 3D/4D printing: A review

Christian Gauss*, Kim L. Pickering, Lakshmi Priya Muthe

School of Engineering, The University of Waikato, Private Bag 3105, Hamilton, New Zealand

ARTICLE INFO

Keywords:
Additive manufacturing
Smart materials
Biobased composites
Functionality
Reinforcement

ABSTRACT

Cellulose is one of the most versatile biopolymers found in nature. Its use is now transitioning from sustainability-focused development to provide technical solutions across a wide range of applications. This review paper describes the use of cellulose as reinforcement in biocomposites and recent related advances in 3D printing technologies, including 4D (responsive/smart) printing and current/future applications. Relevant aspects such as the origin and intrinsic/structural properties of cellulose and cellulose/matrix interaction during processing are discussed. A particular focus is directed to identify opportunities for the development of new cellulose-based composites, formulation requirements for 3D/4D printing, and comprehension of the interplay between rheology, chemistry, and processing. Overall, new materials and technologies based on cellulose have shown promising results for real-life applications, opening new scientific development opportunities and a new generation of sustainable and advanced materials.

1. Introduction

Cellulose is considered the most abundant organic compound available in nature [1,2]. It has been used for more than 150 years as a chemical raw material. However, prior to its discovery as a "sugar of plant cell wall" by the French chemist Anselme Payen in 1838, cellulose-based materials have been used by humans for thousands of years for building, clothing and as an energy source [3].

Cellulose is a macromolecule, generally having a combination of crystalline and amorphous regions [4]. In plants, cellulose acts as the main element for reinforcement and is widely found in all plant tissues. Animal and bacterial cellulose are also present in nature but for other functions, such as serving as a growing medium and protection from external adversities [5,6]. Its unique properties, combined with its general availability and potential as a sustainable material, have brought considerable attention for its use in different applications. Its use in composites has been researched and explored using different cellulose types, i.e. nanofibrillated cellulose, cellulose nanocrystals, wood pulp, regenerated cellulose, and cellulose derivatives [7–14]. Additionally, as a natural, mechanically efficient, and biocompatible material with hygroscopic properties, cellulose and its derivatives have been recognised as useful in the formulation of hydrogels and polymer-based composites (using thermoplastic and thermoset polymers) for structural and stimuli-responsive materials manufactured by additive manufacturing [14–21].

Additive manufacturing, also known as three-dimensional (3D) printing, is effectively a collection of methods based on layer-by-layer or spatial deposition manufacturing technologies in which computer-aided design (CAD) is used to create physical 3D objects [22]. These fabrication methods allow direct production of customised and complex shapes/components using metals, ceramics, polymers, and composites. Additive manufacturing is considered by many people as the next manufacturing revolution [22,23]. 3D printing methods can be classified into five main categories: (1) extrusion-based methods, e.g. fused deposition modelling (FDM)/fused filament fabrication (FFF) and direct ink writing (DIW), (2) photopolymerisation methods such as stereolithography (SLA) or digital light processing (DLP), (3) particle fusion methods such as selective laser sintering (SLS), (4) material jetting (inkjet printing), and (5) binder jetting (indirect inkjet printing, i.e., the binder is deposited onto a powder bed) [21,24,25]. When 3D printed objects respond to external stimuli in a controlled and predictable way, and so could be regarded to having been made from "smart materials" [26–29], they are commonly referred to as having been 4D printed, the extra dimension considered to be relating to changes over time [28,30].

The primary use of cellulose for additive manufacturing has been the development of composites for biomedical applications, such as wound dressing devices, prostheses, and tissue engineering [22,31,32]. It has demonstrated exciting and promising results for 3D printed materials with shape-changing behaviour and as a rheology modifier or reinforcing agent [15,16]. Nature so far provides the best examples of how cellulose is used in a biological material to adapt and respond to environmental changes, such as the hygromorphism of a pine cone and other seed shells triggered by humidity changes [33,34]. By using a

* Corresponding author.
E-mail address: cgauss@waikato.ac.nz (C. Gauss).

https://doi.org/10.1016/j.jcomc.2021.100113
Received 14 December 2020; Received in revised form 23 January 2021; Accepted 25 January 2021

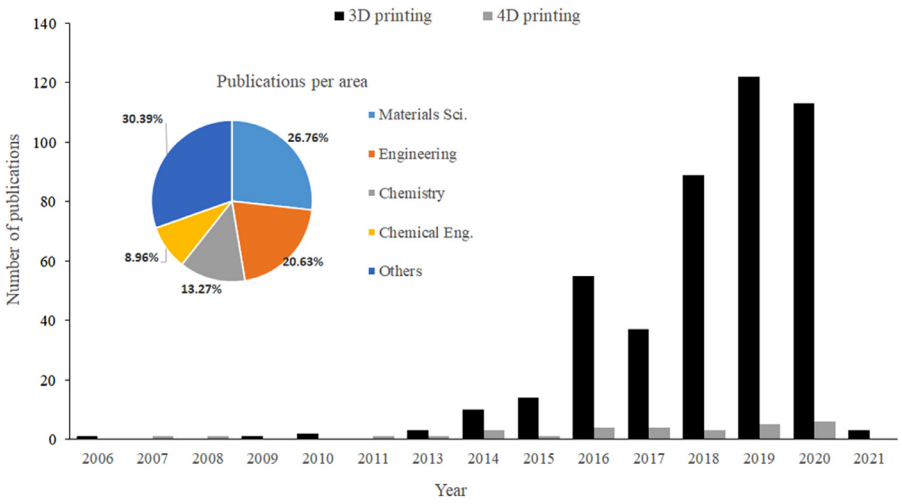

Fig. 1. Number of publications in the Scopus database between 2006 and 2020 with the keywords: "cellulose" AND ("3D printing" OR "additive manufacturing); and "cellulose" AND "4D printing".

biomimetic approach and programming localised anisotropy of cellulose fibrils, precise control of bending and twisting conformations based on shrinking/swelling of cellulose can be achieved [16].

This diverse potential of cellulose is translated into an increased interest in its use for 3D printing in recent years. Indeed, most of the publications related to the use of cellulose for additive manufacturing are concentrated in the last seven years, with a sharp increase in the last three years, as shown in Fig. 1. These publications are mainly distributed in the areas of materials science, engineering, and chemistry, with a total of 477 publications from a staggering number of 48,458 documents related only to the term "3D printing" or "additive manufacturing" in the same timeframe (2006–2021). The United States of America, followed by China, are the countries with the highest number of publications in this field. For the search term "4D printing", there are 516 publications between 2017 and 2021, with only 30 of those publications relating to cellulose.

In this review paper, an overview of cellulose properties and its use for fully bio-derived composites and 3D/4D printing is presented. Different printing methods, formulations, strategies, and related properties are organised as a guideline for future research activities in this promising and recently fledged field of science.

2. Cellulose

Cellulose accounts for approximately 1.5×10^{12} tons of total annual biomass production [3]. It is mainly originated from wood [35], plants or agricultural residues [36], tunicate (animal) [37], algae [38], and bacteria [39–41]. The primary industrial use of cellulose has been the production of pulp and paper, although its use in novel materials, such as inorganic [42,43] and polymeric [9,44] composites, nanocomposites [45], hydrogels [30,46], and even electronics [47,48] have been investigated. Fundamental understanding of cellulose's physical, chemical, and mechanical properties, as well as its crystal structure, has played a pivotal role in further use in novel bio-derived composites [7,9,35]. A brief description of this topic is presented in this section, however, comprehensive reviews can be found elsewhere [5,49,50].

A schematic representation of the wood structure, from the tree to the cellulose elementary fibrils, is shown in Fig. 2(a). Wood has a hierarchical and cellular structure comprised mainly of cellulose, lignin, and hemicellulose (the chemical building blocks) where cellulose microfibrils are organised in defined oriented layers embedded in a hemicellulose and lignin matrix [5,51]. This type of arrangement, also found in other lignocellulosic materials such as palms and bamboo, results in low density and high structural efficiency [52]. Cellulose is composed of a linear chain of ringed glucose molecules with repeat units of two anhydroglucose rings (($C_6H_{10}O_5$)n, where n is 10000 to 15000 depending on the source of the cellulose) linked through oxygen covalently bonded to C1 of one glucose ring and C4 of the adjoining ring, the so-called beta 1–4 glucosidic bond [5,9], as can be seen in Fig. 2(b). These single cellulose chain units compose the elementary fibrils that are organised in crystalline (composed of cellulose nanocrystals) and amorphous (disordered) regions, as schematised in Fig. 2(b) [5].

Crystalline cellulose is polymorphic (I, II, III, IV structures). Cellulose I ($I\alpha$ and $I\beta$) and II are the main forms reported. Cellulose I is considered as "natural cellulose" since it is naturally produced by trees, plants, algae, and bacteria. Its structure can be considered metastable and is usually converted into cellulose II and III depending on how cellulose I is processed [5,53]. Thermodynamically, cellulose II, with a monoclinic structure, is the most stable polymorph with technical relevance (produced by regeneration and mercerisation of cellulose I). The cellulose III is formed from cellulose I and II through liquid ammonia treatments and cellulose IV can be formed by subsequent thermal treatments [5].

Cellulose I presents the highest axial Young's modulus (E) and presents two polymorphs: the triclinic structure ($I\alpha$), space group P_1 ($a = 6.72$ Å, $b = 5.96$ Å, $c = 10.40$ Å, $\alpha = 118.08$ °, $\beta = 114.80$°, $\gamma = 80.375$°) and monoclinic structure ($I\beta$), space group $P2_1$ ($a = 0.778$ nm, $b = 0.820$ nm, $c = 1.038$ nm, $\gamma = 96.5$°) [54,55]. These two polymorphs coexist in different proportions [41]. Cellulose $I\alpha$ is produced by most algae and bacteria, whereas $I\beta$ is the dominant form for plant cell wall cellulose [5].

2.1. Cellulose sources and classification

In general, all plants contain cellulose in their structure, uniquely designed and used to support its own weight and provide sufficient strength to resist external loads caused by wind and rain. However, with a vast infrastructure for planting/harvesting trees and processing, most commercial cellulose is obtained by pulping of softwood or hardwood, in which cellulose is abundant. Hardwoods and softwoods have around 40–47% of cellulose by weight in their composition. Non-wood biomasses, such as cotton, sugar-cane bagasse, coir, sisal, hemp, flax and others, have from 30% (wheat straw) to 95% (cotton) of cellulose [4,56].

Cellulose extraction depends on the structure of the biomass material and the amount of hemicellulose and lignin, the other two main components in plant tissues [5]. Conventionally, isolation of cellulose (pulping), is carried out either by kraft (based on sodium hydroxide and sodium sulphide) or organosolv (ethanol and water) methods. In both of these methods, elevated temperature and pressure are necessary to efficiently remove lignin and hemicellulose [35,57]. After the digestion of the biomass, the resulting cellulose material can be submitted to a sequence of bleaching treatments based on the oxidation of the residual

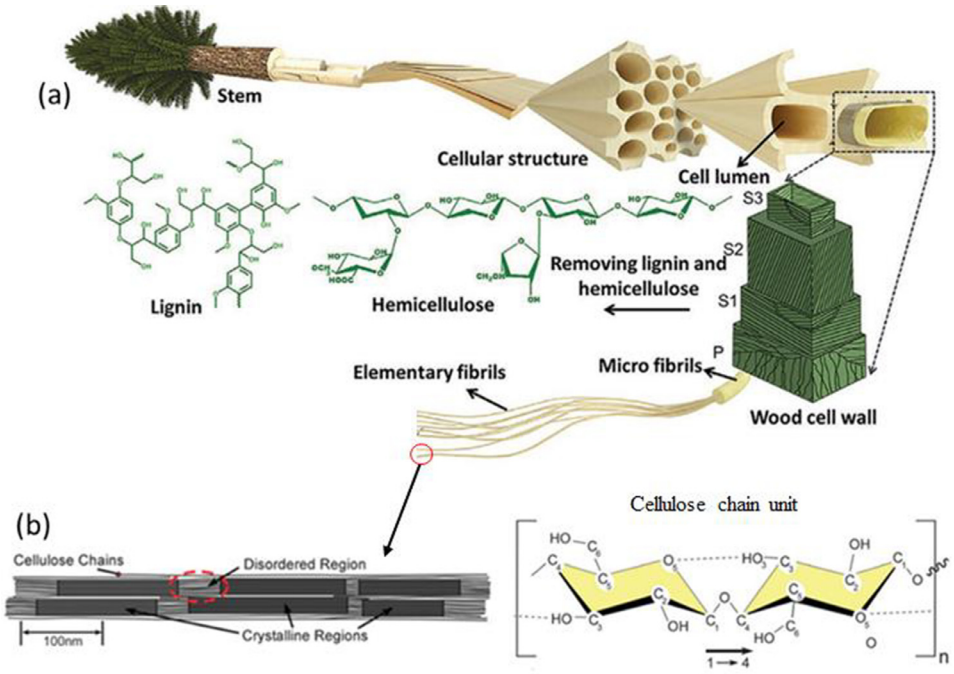

Fig. 2. (a) Hierarchical structure of a tree with a representation of the cellulose organisation within wood. Reproduced with permission from John Wiley and Sons, license number: 4951030836282 [51]. Copyright 2020, John Wiley and Sons. (b) Crystalline (containing cellulose nanocrystals) and amorphous (disordered) regions of elementary fibrils composed of single cellulose chain units (on the right). Reproduced with permission from Chemical Society Reviews, license number:1077823-1 [5].

lignin by chlorine peroxide, hydrogen peroxide, ozone, peracetic acid, or other oxidative agents [35].

Bacterial cellulose, on the other hand, is produced naturally with higher purity and the absence of lignin and hemicellulose; typically, treatments for its use involve culturing methods for cellulose microfibrillar growth and washing steps to remove the bacteria. This type of cellulose can be synthesised by bacteria belonging to the genera *Acetobacter, Rhizobium, Agrobacterium,* and *Sarcina* [58]. These bacteria produce the cellulose microfibrils as a gel with water content as high as 99%. Depending on the culturing conditions, different microfibril formation and crystallisation can be achieved [39,59].

Once cellulose fibres have been isolated, the microfibrillar and/or crystalline components can be separated by additional processing stages. These processes can be conducted by either acid hydrolysis, mechanical treatment, enzymatic hydrolysis, or a combination of two or more of these methods depending on the desired properties [5,60]. The mechanical processes are generally conducted by using high-pressure homogenisers, grinders, cryocrushing, or high-intensity ultrasonic treatments to extract cellulose fibrils. The high shear causes cleavage of elementary cellulose fibrils, producing micro and nanofibrillated fibres. The obtained material can be further processed by chemical treatments to decrease the amount of amorphous cellulose or for surface functionalisation [5,61,62]. Acid hydrolysis is utilised to remove amorphous material and isolate cellulose crystalline particles. Sulphuric acid is widely used for this process because it produces a negative surface charge on the cellulose nanocrystals, which improves the water-dispersibility and colloidal stability [5,63]. The isolated cellulose is also used for the production of cellulose derivatives such as carboxymethyl cellulose, cellulose acetate, cellulose acetate propionate, and nitrocellulose [64] and regenerated cellulose fibres produced by Lyocell or rayon processes [65,66].

According to Moon et al., cellulose fibres can be classified regarding their structure and morphology [5] (complemented with regenerated cellulose fibres). These nomenclatures will be used throughout this review paper:

Cellulose microfibre (MF): Also known as cellulose pulp. Fibres with low crystallinity (43–65%). The dimensions of pulp fibres depend on the biomass. Fibres extracted from wood (softwood or hardwood) and or other plants (bamboo, cotton, sisal, ramie) have length and width in the range of 0.7–25 mm and 8–200 μm, respectively [67–69]. Generally, pulp fibres are the starting materials for the other processed cellulosic materials.

Microcrystalline cellulose (MCC): MCCs are porous particles (10-50 μm diameter), with high-cellulose content and crystallinity, composed of aggregate bundles of hydrogen-bonded cellulose microfibrils. Normally prepared by acid hydrolysis of MF using sulphuric or hydrochloric acid, followed by neutralisation and spray-dried or delivered in a colloidal form [56].

Cellulose nanocrystal (CNC): Also known as nanocrystalline cellulose, cellulose whiskers, nanowhiskers. Depending on the source, plant-derived CNCs are 77–503 nm in length and 5–14.6 nm in width, resulting in aspect ratios of 8.5–100 [70]. CNCs have high crystallinity (54–88%) and a high fraction of Iβ cellulose (68–94%). Produced using similar processes to MCC. CNCs have rod-like or whisker shaped particles after acid hydrolysis of cellulose

Nanofibrillated cellulose (NFC): 100% cellulose with amorphous and crystalline regions. NFCs are compossed of elementary fibrils consisting of 36 cellulose chains arranged in the Iβ crystal structure. High aspect ratio with a square cross-section (4–20 nm wide, 500–2000 nm in length). Produced by mechanical refining of highly purified MF pulps in combination with other techniques to facilitate fibrillation. .
Bacterial cellulose particles (BC): Microfibrils secreted by various bacteria separated from bacterial bodies. BCs are characterised to have a high aspect ratio (higher than 50) with a morphology depending on the bacteria and growing medium. *Acetobacter* microfibrils have a rectangular cross-section (6–10 nm by 30–50 nm). Primarily composed of Iα structure.

Regenerated cellulose (RC): Regenerated cellulose has a cellulose II structure and is produced by derivatising (Viscose) or direct dissolution (Lyocell) of MF, or other sources of cellulose [71]. The RC fibres are produced continuously with a diameter ranging from 10 to 36 mm [10,72,73]. The main application is textiles [71].

2.2. Cellulose mechanical properties

The mechanical properties of cellulose fibres play an essential role in the development of new composites. Cellulose from different origins has similar chemistry, but, variations in the morphology, type, and crystal structure result in different mechanical properties. The mechanical

Table 1
Mechanical properties cellulose fibres. Adapted from [5].

Material	E_A (GPa)	E_T (GPa)	σ_f (GPa)	ϵ_f (%)	Method	Ref.
MF	14–27	-	0.3–1.4	4–23	Tensile	[75]
MCC	25 ± 4	-	-	-	Raman	[74]
CNC						
Plant	57-105	-	-	-	Raman	[76]
Wood		18-50	-	-	AFM indentation	[77]
BC	78 ± 17		-	-	AFM-3pt bend	[78]
	114		-	-	Raman	[79]
Cellulose Iβ						
Experimental	120-135		-	-	XRD	[80]
	220 ± 50	15 ± 1	-	-	IXS	[81]
Modeling	137-168	10-50	7.5-7.7	-		[82,83]
Cellulose Iα						
Modelling	128-155	5-8	-	-		[83,84]
Cellulose II			-			
Experimental	9–90		0.2–1.0	-	Raman	[85,86]
Modeling	98–109	17–31	4.9–5.4	-		[83,85,87]
RC (Cellulose II)						
Viscose	11–20	-	0.39–0.83	-	Tensile	[10]
Lyocell	9–12.5	-	0.55–1.01	-	Tensile	[10]; [73]

E_A=Axial Young's modulus; E_T=Transverse Young's modulus; σ_f =tensile strength; ϵ_f = failure strain

properties are also dependent on the cellulose crystallinity; the more crystalline, the stronger the cellulose fibre [74]. Indirect methods, such as X-ray diffraction, Raman spectroscopy, or atomic force microscopy (AFM), and simulations are generally used to infer the Young's modulus or strength of micro and nanosized cellulose fibres. With a density of 1.6 g/cm^3, crystalline cellulose is considered to have the highest specific stiffness among naturally produced materials, with estimated values in the order of 67-137 GPa cm^3.g^{-1} [5,52]. Table 1 gives an overview of the tensile properties of different types of cellulose, from the nanofibres up to microfibres, and regenerated cellulose.

3. Cellulose-based biocomposites

Lignocellulosic fibres have been used widely in polymeric-based composite formulations. Availability, high specific mechanical properties, and sustainability are the main reasons for their use [88]. A wide range of natural fibres, such as hemp, sisal, bamboo, flax, curaua, and jute is commercially available. The use of these natural fibres has increased steadily in the last years, with a particular interest in the automotive industry [89]. Generally, both petroleum-based and bio-derived polymers are used as matrices for natural fibre composites. Although petroleum-based thermoset polymers such as epoxy and polyurethane (PU) and thermoplastics such as polypropylene (PP), polyethylene (PE), and acrylonitrile butadiene styrene (ABS) have been successfully applied for the manufacturing of NFCs with good mechanical and physical properties, these matrices still leave challenges to achieve genuinely sustainable materials. The recyclability potential of natural fibre composites [90,91] and the use of biodegradable thermoplastic polymers such as polylactic acid (PLA), polyhydroxyalkanoates (PHA), polyglycolic acid (PGA), starch, and bio-derived thermosets such as bioepoxy resins (acrylated epoxidised soybean oil; BioPoxy 36©; DGEDP-ethyl ester) in combination with other bio-derived materials are paving the path for new for commercial applications [92–96]. A comprehensive review of the general use of lignocellulosic fibres for composites is presented elsewhere [88,97,98].

In this review paper, we focus mainly on the use of cellulose fibres, i.e. those of high cellulose content, extracted from a lignocellulosic source (through chemical and/or mechanical processes) or obtained by bacterial cultures and their use in combination with bio-derived polymers for composite formulations and additive manufacturing. Cellulose and nanocellulose-based composites have been used for different technological applications, such as sustainable packaging, water treatment, CO_2 capture, sensors and flexible electrodes, flexible supercapacitors, tissue engineering [99], and as a structural material. A series of meaningful review papers have been published addressing the use of cellulose for composites and nanocomposites [4,5,9,35,56,61,100,101], stimuli-responsive materials [102,103], and hydrogels and aerogels [7]. The main interest in using cellulose for new materials development has been the improvement of physical (e.g., thermal stability, water vapour transmission, and rheology) and mechanical properties (e.g., tensile strength, Young's modulus, and toughness) of polymeric matrices.

As an overview of the latest achievements in terms of cellulose-reinforced composites, Fig. 3 summarises the tensile strength and Young's modulus of cellulose-based composites published in the last twenty years. Only formulations completely bio-derived and the best tensile properties achieved in each publication have been included. Additional information relating to these results (failure strain and manufacturing method) is given in Table 2. Different types of cellulose, e.g., NFC, CNC, MF, BC, RC, have been used for the manufacturing of composites by different methods. There has been considerable attention in PLA-based formulations, with a continuous effort in improving their mechanical and physical performance [12,72,92,104–118]. This is explained considering that PLA is known as the first mass-produced biopolymer with potential to replace commodity thermoplastics for a diversity of applications, from biomedical to packaging applications [110]. Regarding thermoplastics, the best tensile performance of cellulose-reinforced composites has been achieved by using PLA as a matrix. Nevertheless, fragility, low impact strength and thermal stability still are issues reported in PLA-based composites. Other thermoplastic matrices have also been successfully reinforced with cellulose, achieving properties comparable to those of PLA-based composites [110,117,119,120].

Despite the high-potential of cellulose for reinforcement owing to its outstanding mechanical properties (Table 1), there are still many unsolved hurdles for the development of cellulose-based biocomposites, which have been limiting the mechanical properties improvement of biocomposites. The inherent hydrophilicity of cellulose is the main challenge for the development of composites [99], as it affects its dispersibility and interfacial bonding with the matrix. Different routes have been attempted to physically or chemically alter cellulose's surface and improve its compatibility with hydrophobic matrices (most of the available biopolymers). The interfacial bonding between cellulose and the matrix can be improved by using nanosized forms of cellulose (bacterial cellulose, NFC, CNC), providing an increased surface area per volume. However, chemical incompatibility remains, causing limited dispersion of cellulose within the composites. Therefore, different strategies have also been used to chemically modify micro and nanocellulose fibres and

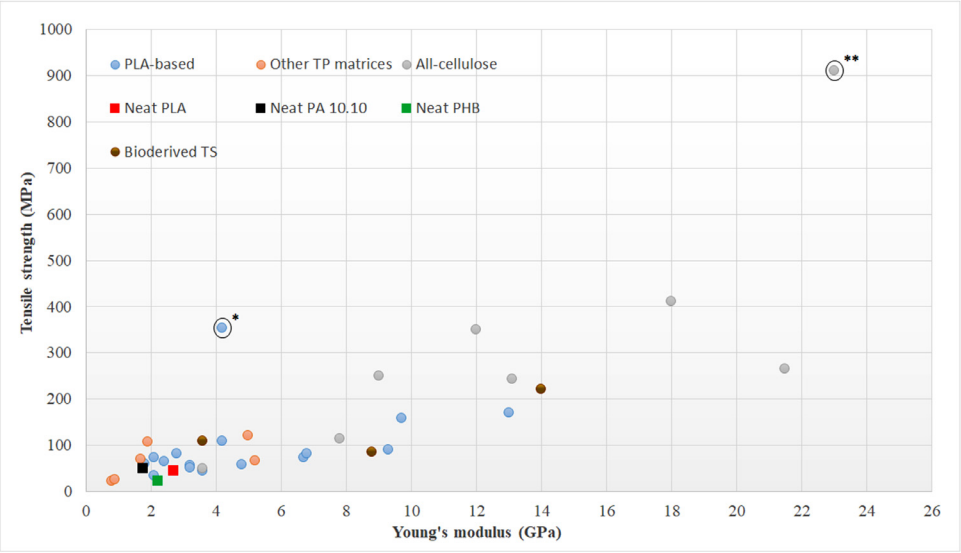

Fig. 3. Overview of the tensile properties of bio-derived composites reinforced with different types of cellulose, matrices and processing methods; TP – Thermoplastic, TS – Thermoset. Data extracted from papers published between 2001 and 2020 [12,72,92,104–127]. *Values of PLA-based composite produced by solid-state drawing [111]; **Values of all-cellulose composite produced using Bocell fibres [126].

Table 2
Overview of different types of cellulose and processes used for the composites. Data presented in Fig. 3. Extracted from papers published between 2001 and 2020 [12,72,92,104–127].

Matrix	Cellulose type (reinforcement)	Tensile strength (MPa)	Young's modulus (GPa)	Failure strain (%)	Manufacturing methods
PLA	RC	58–158	4.2–9.7	4.1-5.8	IM; CM
	CNC	50–353*	1.8–4.2*	4-187	FC; IM; CM
	MF	61–65	2.4-6.8	3.4	IM; FC
	NFC	33–170***	2.1–13***	1.5–189	FC;CM
Other matrices (PA 10.10; PHB; PHA; PVA/Chitosan; PBS/PLA)	RC	66–120	5–5.2	–	IM; CM
	CNC	73–107	1.9–2.1	30	FC
	MF	25	0.9	3.8	FC
	NFC	69	1.7	298	CM
Bio–derived thermosets (Epoxies; Lactic acid/glycerol)	RC	220	14	4	CM
	NFC	108	3.6	4.8	RI
	BC	84	8.8	1	RI
All–cellulose	RC	264–910**	7.8–23**	8.2–24	SD; SI/CM
	CNC	49	3.6	2.1	FC
	MCC	243	13.1	10.7	FC
	BC	411	18	4.3	SD

Where:IM – Injection moulding; CM – Compression moulding; FC – Film casting; SI – Solvent infusion; SD – Selective dissolution; RI – Resin infusion. *Produced by solid-state drawing [111]; **Produced using Bocell fibres [126]; ***Produced by using PLA fibres [115].

improve their compatibility with polymeric matrices, such as acetylation [92,128], esterification [109] and grafting [12,104,107,108,129]. The hydrophobic surface modification has been considered one of the best routes to improve cellulose dispersion and interfacial bonding. Other routes, such as Pickering stabilisation strategy (emulsion stabilised by nanocelluloses that are adsorbed onto the interface between two immiscible phases) and brick-and-mortar arrangement (structure based on mimetics of biological materials, e.g., nacre, shells, and bones) approach, have also demonstrated promising results for high-performance materials [99].

In thermoplastic composites, acetylation modification of NFC has been demonstrated to be a viable solution to improve the mechanical properties. Formulations of PLA nanocomposites with up to 5% of acetylated NFC presented considerable improvement in Young's modulus, tensile strength, and failure strain [92]. With 1% of modified NFC, the failure strain was increased by more than 60%. Samples with 3% of NFC were found to have the best tensile strength (33 MPa) and failure strain (189%), with improvements of 118% and 372%, respectively, compared to neat PLA [92]. Grafting of polymers and other functional groups onto cellulose surface is also supported as a promising strategy. Grafting CNC with triazine derivative enhanced the strength and failure strain of PLA-based composites, in comparison with neat PLA and unmodified CNC [108]. Lactic acid (precursor of PLA) was also grafted onto cellulose fibres extracted from bamboo, improving their compatibility with PLA and resulting in 19% increase in tensile strength and 30% in failure strain, compared to composites produced with untreated fibres [129]. The combination of cellulose surface treatment by in situ polymerisation and a new processing route to manufacture PLA-based films resulted in outstanding mechanical properties. Small amounts (up to 0.3%) of CNC modified by in situ emulsion polymerisation of methyl methacrylate (MMA) was used in PLA composites by melt compounding through liquid-assisted extrusion [111]. By using hot pressing followed by solid-state drawing at 100 °C, films with aligned CNC were found to have a tensile strength of 353 MPa, Young's modulus of 4.2 GPa and failure strain of 45.7%. These promising mechanical properties are explained mainly by the decrease in the PLA crystallites and their sliding effect after solid-state drawing [111].

Biobased thermoset polymers have also been reinforced with cellulose. A biobased epoxy, diglycidyl ether diphenolate ethyl ester (DGEDP-ethyl), was used for composites reinforced with up to 30% of bacterial cellulose, which resulted in a 7-fold increase in Young's modulus and 35% increase in tensile strength in comparison with neat epoxy. The addition of BC also improved the thermo-mechanical performance and thermal stability of the composite [95]. NFC was also successfully ap-

plied in a commercial biobased epoxy resin as reinforcement. With 13-23% of NFC in the form of films, the resulting maximum tensile strength (108 MPa), Young's modulus (3.6 GPa), and failure strain (4.8%) of the composites were improved by 74%, 56%, and 65%, respectively. Additionally, the addition of NFC reduced the water vapour permeability and did not affect the thermal stability of the epoxy matrix. Another thermoset resin based on lactic acid, glycerol, and methacrylic anhydride was also applied in the formulation of cellulose-reinforced composites. With 75% of viscose fibres in the form of textiles as reinforcement, better mechanical properties than those reported in cellulose-reinforced PLA composites were obtained, achieving a tensile strength above 200 MPa, Young's modulus of up to 14 GPa, and failure strain between 3–5%, depending on the type of textile used in the formulation [130].

As in thermoplastic-based composites, chemical modification of cellulose fibres is also explored to improve mechanical and physical properties of thermoset composites. By treating microcrystalline cellulose (MCC) through an esterification reaction with methacrylic anhydride (MAA), successful crosslinking with acrylated epoxidised soybean oil (AESO) was achieved [131]. The use of modified MCC resulted in a significant improvement in flexural strength (up to 67.2%), modulus of elasticity (up to 77%), water resistance, glass transition temperature (Tg), and interfacial bonding. The composites obtained, however, are very flexible (modulus of elasticity in the order of 400 MPa) and limited to non-structural use.

As shown in Fig. 3/Table 2, the best mechanical properties of biobased composites are achieved by all-cellulose formulations. All-cellulose composites (ACC) are a new class of monocomponent composites that are obtained mainly by non-derivatising methods, i.e., the cellulose chemical structure is not altered after solubilisation/regeneration [132]. Non-derivatising solvents like lithium chloride/N,N-dimethylacetamide (LiCl/DMAc), dinitrogen tetroxide/dimethylformamide (N_2O_4/DMF), N-methylmorpholine-N-oxide (NMMO), mineral acids, NaOH/Urea, dimethylsulfoxide/tetrabutylammonium fluoride (DMSO/TBAF), dimethylimidazolone/lithium chloride, and various molten salt hydrates and ionic liquids (ILs), can be used to dissolve cellulose [132]. LiCl/DMAc, NMMO, NaOH/Urea and the IL 1-butyl-3-methylimidazolium chloride (BmimCl) are the main solvents reported. Two distinct methods can be used to produce ACCs; a 2-step method where firstly a portion of cellulose is dissolved in a solvent and then regenerated in the presence of undissolved cellulose [122]; and a 1-step method where the surface of cellulosic fibres are partially dissolved and then regenerated in situ to form a matrix around the undissolved portion [133]. Through a process of selective dissolution of regenerated cellulose by a LiCl/DMAc solution, the highest mechanical properties reported so far for biobased raw materials have been achieved [126]. By using Bocell fibres, regenerated cellulose with high crystal alignment, the authors reported a tensile strength of up to 910 MPa and Young's modulus of 23 GPa with a failure strain of 8%. To the best of our knowledge, there is no other biobased laminated composite with such mechanical properties. It is worth mentioning that all-cellulose composites are completely biodegradable, with similar behaviour to native cellulose [134].

4. The use of cellulose for additive manufacturing

The diversification of the use of cellulose has been continuously increasing over the last several decades. It has been suggested that there have been a number of generations of technological developments for cellulose that have supported different applications of which we are now in the fifth generation. Fig. 4 summarises the relationship between the technological development and diversification of cellulose-based products according to these five generations [60]. The first generation was based on the use of cellulose, mainly cotton, as a fibre source for exploitation in textiles. In the second and third generations, chemical processes were introduced, which made possible the isolation of cellulose from wood and cotton for the production of paper and cellulose derivatives for use in pharmaceutical, cosmetics, food, and healthcare applications. The fourth generation is characterised by the exploration of cellulose composition at a molecular level for biochemicals, biofuels, and biopolymers by using different lignocellulosic sources. Finally, for the fifth generation, through exploring and characterising cellulose in the nanoscale, the use of nanocelluloses has been identified as a technical solution for additive manufacturing, packaging, construction, automotive, biosensors, smart materials, and many other emerging technologies.

The use of bio-derived materials in additive manufacturing is increasing with the constant demand in innovation for sustainable materials and circular economy requirements within the manufacturing industries [135]. Polymers and in particular, thermoplastics, are the most commonly used materials for additive manufacturing, with fused deposition modelling being the most used method [136]. The reasons for preferring polymers over other materials in additive manufacturing are that they are versatile, available with a variety of physical and chemical properties, easy to handle because of relatively low working temperatures, and are economical [137,138].

Although polymers have been the most preferred materials for 3D printing, extensive use of petrochemical polymers does not align well to achieving a circular economy. Despite the recyclability potential of petrochemical thermoplastics [139], bio-derived raw materials can be locally produced from a variety of crops such as sugarcane, potatoes, maise, sugar beet, perennial grass, and crop residues [135], which virtually enable a circular production chain (extraction, processing, usage, disposal/reuse/recycle) in most parts of the globe. Hence, there has been a significant amount of research towards incorporating bio-derived polymers and their composites as alternatives for conventional oil-based polymers to make the additive manufacturing industry more sustainable [140].

The use of cellulose for 3D printing composites formulations has started to be reported in the last decade. The main advantage of cellulose for 3D printing is related to its high aspect ratio, availability, processability, sustainability (although in many cases, intense chemical processes are used), and suitability for chemical functionalisation. Its combination with other bio-derived polymers such as gelatines and alginates has been extensively investigated for the formulation of aerogels [141,142] and hydrogels [20,143–146] for 3D printing, extending the use of cellulose in medical, tissue engineering, wearables, electronics, and load-bearing applications [16,20,147,148]. Recent progress has also been achieved in 3D printing of all-cellulose composites with outstanding properties by using either pure dissolved cellulose [149] or cellulose derivatives, such as carboxymethyl cellulose (CMC), methylcellulose (MC), ethyl cellulose (EC), hydroxyethyl cellulose (HEC), hydroxypropyl cellulose (HPC), and hydroxypropyl methylcellulose (HPMC) [21]. Furthermore, potential has been seen in the area of 4D printing by using cellulose in situations where stimuli-responsive behaviour is an advantage [16,20,150].

4D printing utilises smart materials that are programmed to exhibit changes in one or more properties in a controlled manner on the application of an external stimulus [151]. To achieve an appropriate response in a 4D printed material, selection of external stimulus plays an important role. Many researchers have used stimuli such as heat, water, and light to achieve a controlled response from a printed product [152]. Cellulose has been mainly used as the component to provide shape-changing characteristics to 4D printed objects by its anisotropic shrinkage/swelling behaviour with the variation of moisture. The combination of this intrinsic property, the possibility of alignment during printing, and 3D modelling/prediction enable the use of cellulose as a 4D printing material [16,150]. Other fillers such as nanoclays can be added to cellulose-based composites to improve storage stability and printability of hydrogels and create a moisture-responsiveness behaviour upon hydration and dehydration [20].

The wide range of cellulose-based compounds available with different shapes, sizes, and properties, enables the use of cellulose for different purposes in 3D printing: rheology modifier, binder, excipient, matrix,

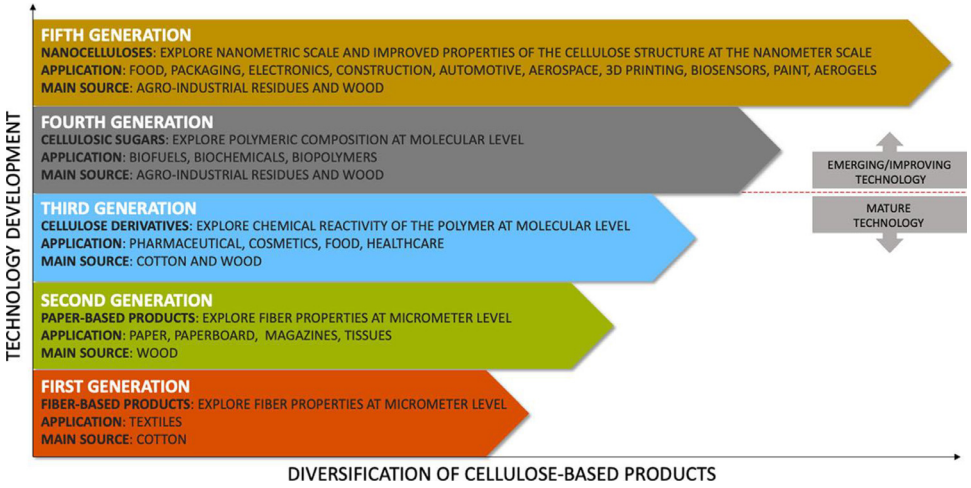

Fig. 4. Diversification of cellulose products according to technological development. Reproduced with permission from Springer Nature, license number: 4951050511433 [60].

Table 3
Uses of cellulose in 3D printing (adapted from [21,153,154]).

Use of cellulose	Properties that enable the use of cellulose	Application in 3D printing
Rheology modifier	Neighbouring chains in cellulose form hydrogen bonds, restricting the water motion and increasing the viscosity. At a high shear rate, hydrogen bonds break through shear thinning behaviour.	Cellulose has suitable rheological properties for 3D inks as the ink flows smoothly at high shear rates and quickly solidifies once the printing stops.
Binder	Cellulose has shear thinning behaviour making it a good choice of binder for 3D printing powders	Rheology of a 3D printing paste depends on the rheology of a binder. Shear-thinning property of the cellulose binder helps in achieving a successful print.
Excipient	Hydrophilic nature of cellulose helps achieve controlled swelling on contact with water.	This property of cellulose can be exploited in applications such as drug delivery and 4D printing
Matrix	High molecular weight cellulose dissolved by solvents has a high viscosity and exhibits shear thinning.	High viscosity solubilised cellulose is suitable for 3D printing methods such as material extrusion method to produce dimensionally stable prints
Reinforcement	Cellulose fibres exhibit high strength, high stiffness, and low density	Cellulose fibres extruded with thermoplastics are commonly used as filaments or used in bioink formulations. 3D printed cellulose-based composites have shown improved mechanical properties

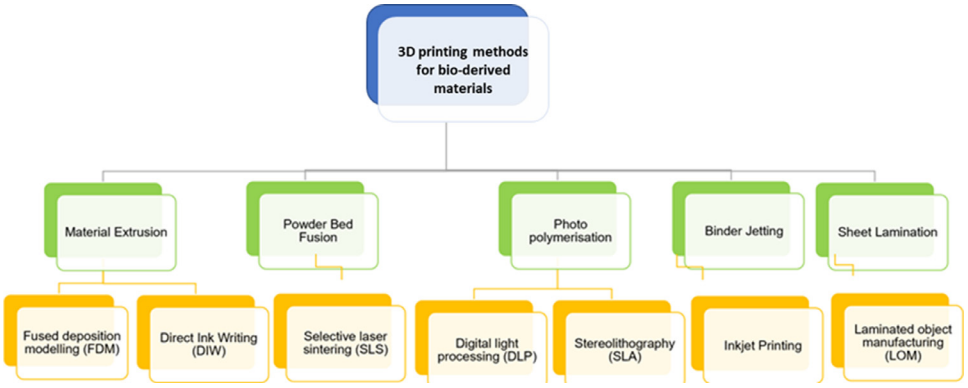

Fig. 5. 3D printing methods used for bio-derived materials (adapted from [155] and [156])

and reinforcement [21,153,154]. Table 3 gives a summarised overview of the uses of cellulose for 3D printing and related properties and applications. This arsenal of possibilities for cellulose in additive manufacturing has remarkably increased the interest of the scientific community in improving, developing and characterising new processes and materials, as described in details in the next sections.

4.1. 3D printing methods for cellulose-based biocomposites

Biocomposites are processed by a variety of 3D printing technologies, including extrusion, powder bed fusion, photo-polymerisation, binder jetting, and sheet lamination methods (Fig. 5). Material properties and desired structural resolution determine the type of 3D printing method to be used [155,156].

Extrusion based methods are the most used 3D printing methods for biocomposites. Usually, short natural fibres are mixed with polymer pellets and extruded to obtain a biocomposite filament for FDM. FDM can also be used for 3D printing thermoplastic composites with long natural fibres[130]. Micro/nano cellulose fibres have been widely used as reinforcements in FDM as they have proven to improve mechanical properties of the printed samples.

DIW, an extrusion-based 3D printing method, also referred to as liquid deposition modelling, direct paste writing or paste extrusion [157,158], is mostly used for printing gels/inks. Cellulose-based sus-

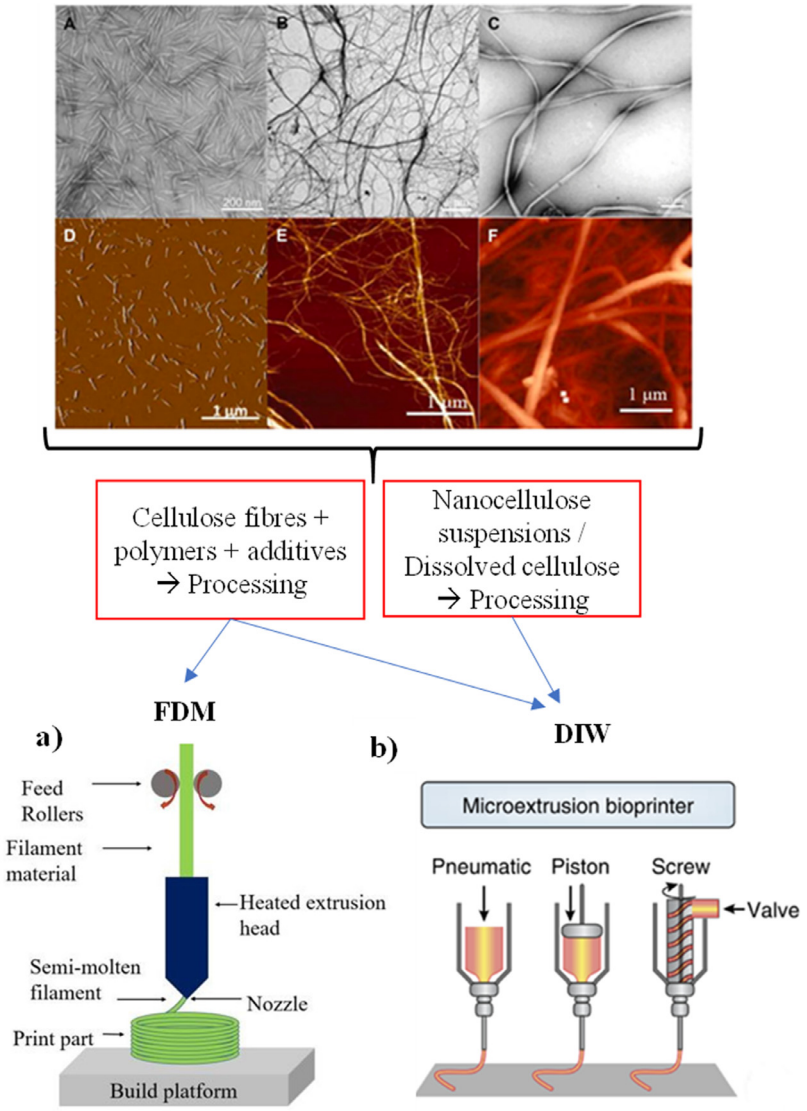

Fig. 6. Images of different types of cellulose (CNC (A/D); NFC (B/E); BC (C/F)) used for composites formulations obtained by TEM (A-C) and AFM (D-E). Reproduced with permission from Elsevier, license number: 4951050961201 [162]. Original TEM and AFM images: A: Reproduced with permission from Springer Nature, license number: 4951051407570 [164]; B: Reproduced with permission from Springer Nature, license number: 4951060668766 [167]; C: Reproduced with permission from Elsevier, license number: 4951051258417 [163]; D: Reproduced with permission from Springer Nature, license number: 4951060510823 [166]; E: Reproduced with permission from [168]. Copyright 2014, American Chemical Society; F: Reproduced with permission from Elsevier, license number: 4951060063149 [165]. Bottom: the two most used methods of using cellulose in 3D printing, a) FDM method [169] and b) liquid extrusion or DIW used in bioprinting, reproduced with permission from Springer Nature, license number: 4951061346314 [170].

pensions with shear-thinning behaviour have been 3D printed using DIW method for applications including biomedical and tissue engineering [24]. Rheological characteristics of cellulose-based colloidal suspensions play an important role in 3D printing. Stability of viscous behaviour with respect to temperature is vital to prevent viscous flow ink and collapse of the printed material. Much work has been done in understanding colloidal stability and coagulation issues while 3D printing aqueous suspensions [159].

Cellulose is also being used in photopolymerisation 3D printing methods, conventionally as a complementary step in DIW, with applications in biomedical engineering. The primary purpose of using cellulose in photo polymeric resins is to improve mechanical properties and thermal stability of the 3D printed product [157]. Stereolithography (SLA) and digital light processing (DLP) are other printing methods used in the biomedical field to print cellulose-based biocompatible photoreactive resins. Applications such as bone cement, bone substitutes, and drug delivery systems could incorporate biocompatible cellulose-based photosensitive resins as an alternative of methacrylate-based resins that are used currently [24,160,161].

Although different printing methods have been used for cellulose-based formulations, as previously mentioned, most of the studies on this topic focused on extrusion-based methods such as the use of thermoplastics (using FDM) and inks or gels (DIW), as schematised in Fig. 6.

4.2. The use of cellulose in thermoplastics

The properties and processability of filaments with natural fibres/fillers for FDM have been extensively reviewed [171–175]. However, although research in bio-derived polymers and their composites involves different materials, commercially available bio-derived filaments are limited to PLA blends with wood-based materials.

Tables 4 and 5 give an overview of the methodology and main findings of recent developments in 3D printing with the use of cellulose in thermoplastic composites using FDM. Most of the research with bio-derived biocomposites has been concentrated on the use of PLA as the matrix. The main reason for this choice is the combination of good mechanical properties, processability, printability, availability, and price, as previously discussed. Therefore, PLA is one of the most used bio-derived polymers for 3D printing technologies and is well consolidated in the market [172]. Around 65 entries related to commercial PLA for FDM can be found in the Senvol Database for 3D printing materials with a range of physical-mechanical properties [176]: Glass transition temperature (Tg) between 55–63 °C; apparent density between 1.20–1.27 g/cm^3; tensile strength between 27–145 MPa; Young's modulus between 1.77–4.00 GPa. Although other biopolyesters are commercially available, e.g., polybutylene succinate (PBS), polybutylene adipate-co-terephtalate (PBAT), and polybutylene succinate-co-adipate

Table 4
Summary of different formulations, processing and printing conditions of recent developments in cellulose-based composites for fused deposition modelling.

Year	Cellulose source and content (%)	Matrix	Compounding and filament production	Printing parameters	Reference
2017	NFC (1–5%)	PLA	NFC grafted with L-lactide mixed with PLA by solvent casting and then extruded with neat PLA in a kinetic blender at 180 °C and 30 RPM. Filaments of 1.75 mm were produced in a single screw extruder at 165 °C.	Filament not tested in 3D printing.	[181]
2017	TMP - thermomechanical pulp (10–20%)	PLA	Dry mixing of ground TMP fibres and PLA followed by two extrusions of filaments with 2.2 mm in a single screw extruder at 165-175 °C.	Ultimaker Original 3D printer. Temperature of 210 °C at 15 mm/s with a nozzle diameter of 0.4 mm.	[182]
2018	Nanocellulose (NC) (0.5–3%)	PLA and PHBH	Masterbatch with 10% NC by solvent casting with chloroform. Melt compounding in a single screw extruder at 30 RPM and 190 °C (PLA) and 150 °C (PHBH)	Sharebot Next Generation desktop 3D printer. Temperature of 210 °C for PLA and 180-200 °C for PHBH with a nozzle 0.35 mm. 100% of fill rate.	[186]
2018	MCC - microcrystalline cellulose (1–5%)	PLA	Solvent casting of PLA/MCC in tetrahydrofuran (THF) followed by dry mixing with neat PLA. 1.55 and 1.75 mm filaments extruded in a twin screw extruder at 65 RPM at a temperature profile of 165 – 190 °C.	AutoMaker, Robox 3D printer (no information regarding printing parameters).	[187]
2019	NFC (10-40%)	PLA	NFC added to PLA dissolved in chloroform, dried, and compounded in a high shear mixer. Filaments of 1.68 mm were produced in a plunger-type batch extruder.	Commercial desktop FDM unit (Solidoodle 3 from Solidoodle Co). Temperature between 180-215 °C, nozzle of 0.4 mm, layer height of 0.2 mm and printing speed between 7.5-15 mm/s	[180]
2019	BC – bacterial cellulose (1–2.5%)	PLA	Composites prepared by Pickering emulsion method. TEMPO oxidised BC dispersed in water was mixed with PLA dissolved in DCM. After obtaining a Pickering emulsion by high intensity mixing, the DCM was evaporated and the resulting particles filtered. The obtained particles were extruded in a single screw extruder at a temperature profile of 180-195 °C	Funmat HT 3D printer. Temperature of 220 °C (bed temperature of 60 °C) at 75 mm/s with a nozzle of 0.4 mm. Infill degree of 100%.	[183]
2020	NFC (1-5%)	PLA	Melt compounding in a single screw extruder at 35 RPM. Nominal filament diameter of 1.75 ± 0.05 mm	M3036FDM desktop 3D printer. Temperature of 210 °C at 40 mm/s with a nozzle of 0.4 mm. 10% and 35% of fill rate.	[179]

(*continued on next page*)

Table 4 (*continued*)

Year	Cellulose source and content (%)	Matrix	Compounding and filament production	Printing parameters	Reference
2020	NFC (1–5%)	PLA	Solvent casting method: NFC dispersed in DMF and mixed with PLA dissolved in chloroform. Filaments of 1.75 mm produced in a capillary rheometer at 180 °C at speed of 0.2 mm/s.	Formulation with 1% of NFC printed in a Fracktal works - Julia V2 desktop 3D printer. Temperature of 180 °C (bed temperature of 60 °C) at 45 mm/s with a nozzle of 0.6 mm. Infill degree of 100%	[188]
2020	Nanocellulose (1–5%)	PLA	Dry mixing of nanocellulose and PLA particles followed by extrusion of 1.75 mm filaments in a single screw extruder at 75 °C and speed of 25 rpm.	Filament not tested in 3D printing.	[189]
2020	CNC (5–10%)	PHBH	Solvent casting method: CNC dispersed in chloroform (after solvent exchanging) and mixed with PHBH dissolved in chloroform. The obtained material was melt compounded in a high-shear mixer and the filaments of 1.75 mm were produced in a capillary rheometer at 145 °C.	Filaments 3D printed in a Vellemen K8200 3D printer at 170 °C, speed of 5 mm/s, and nozzles of 0.6 and 0.4 mm. Infill degree of 100%	[178]

PHBH: Poly(3-hydroxybutirate-co-3-hydroxyhexanoate)

(PBSA), PLA has the most appropriate combination of physical and mechanical properties for 3D printing applications [177].

The main focus in using cellulose for FDM filaments has been the improvement of the overall mechanical properties of 3D printed constructs. Different strategies have been explored to incorporate cellulose fibres in 3D printing filaments. Generally, reinforced filaments are produced by either melt compounding through extrusion processes or by mixing fibres and polymers by solvent casting followed by melt compounding, as described in Table 4. Most of the studies used nanocelluloses (CNC or NFC) as a source of reinforcement, with contents varying between 1–40%. Improvements of up to 84% in tensile strength and 190% in stiffness were reported. In some cases, there was no positive effect on the mechanical properties by adding cellulose. However, other improvements, such as thermo-mechanical stability and biodegradability rate, are observed [178].

In a recent work, NFC produced by enzymatic hydrolysis of MCC followed by high-pressure homogenisation was applied as reinforcement in PLA filaments for 3D printing [179]. Polyethylene glycol 600 (PEG600) was used as a plasticiser, obtaining good processability of the formulations with up to 5% of NFC. The tensile strength and failure strain of the filaments were improved by approximately 20% and 50%, respectively, compared to neat PLA. This maximum improvement was obtained with 2.5% of NFC while the addition of 5% had limited improvement [179]. In another study, up to 30% of NFC was used in PLA filaments resulting in improvements of up to 45% in tensile strength and 130% in Young's modulus in 3D printed samples [180]. However, reductions in the failure strain and toughness were observed, and the 3D printed samples presented inferior properties than those of compression moulded counterparts.

The agglomeration of nanocellulose (heterogeneous dispersion), reduction in toughness, and difficulties in processing have been the main problems reported in recent papers. The success of using cellulose for reinforcement lies in the combination of four main aspects: dispersion, interfacial bonding, alignment, and aspect ratio of the fibres. Alignment and aspect ratio of the fibres are usually controlled by processing conditions and proper fibre selection, whereas interfacial bonding and dispersion improvements demand additional chemical/physical treatments, generally conducted by surface treatments.

Although the effect of surface modifications on the dispersion and interfacial bonding of cellulose in hydrophobic matrices is limited, remarkable improvements have been achieved [162]. By using a strategy of polymer grafting onto NFC fibres, L-lactide was used for a liquid assisted in situ polymerisation reaction to improve the interfacial bonding and dispersion of NFC in PLA. The grafting was successfully verified by transmission electron microscopy (TEM), X-ray photoelectron spectroscopy (XPS), and Fourier-transform infrared spectroscopy (FTIR) analyses. The combination of grafting treatment and annealing (120 °C) above the cold crystallisation temperature (Tcc), resulted in 66% increase in tensile strength and 28% in stiffness with 3% of PLA-g-NFC [181]. The addition of modified cellulose did not change the Tg, but decreased the cold crystallisation temperature (Tcc), facilitating the crystallisation of PLA.

Other possibilities for cellulose grafting have been investigated to produce FDM filaments. Filgueira et al. explored an innovative way to functionalise thermomechanical pulp (TMP) fibres by enzymatic-assisted grafting of octyl gallate (OG) and lauryl gallate (LG). The modification of the fibres resulted in considerable hydrophobic properties, reducing the water absorption of the filaments with OG-treated cellulose. The OG grafting also improved the stress transfer between the fibres and the matrix, resulting in better mechanical properties, especially after printing. The best strength was achieved by filament with 10% of OG-grafted fibre, with less than 10% of improvement in comparison with neat PLA. However, 3D printed samples with 20% of OG-grafted fibres had an increase of approximately 190% in tensile strength. Although not

Table 5
Summary of the main findings of cellulose-based composites for fused deposition modelling (related to Table 4).

Year	Cellulose source and content (%)	Matrix	Other materials / cellulose treatment	Observation	Mechanical properties / Other findings	Ref.
2017	NFC (1-5%)	PLA (4032D)	Grafting of NFC through in situ polymerisation of L-lactide (PLA-g-NFCs)	Better dispersion and increase in crystallinity were achieved by grafting the NFCs. Enhanced storage modulus with the addition of PLA-g-NFCs	Tensile testing of the filaments: up to 66% increase in strength and 28% in stiffness with 3% of PLA-g-NFCs (after annealing at 120 °C)	[181]
2017	TMP - thermomechanical pulp (10-20%)	PLA (4032D)	Enzymatic treatment of thermomechanical pulp for laccase-assisted grafting of octyl gallate (OG) and lauryl gallate (LG)	The grafting of LG reduced the water absorption of the filaments and provided hydrophobic properties for the TMP fibres. However the interfacial adhesion between the fibres and PLA matrix was not improved. Using OG, there was an increase in fibre/matrix bonding and increased the water contact angle of the fibres	Decrease in tensile strength of filaments with untreated and LG grafted TMP. Best strength achieved by filament with 10% of TMP grafted by OG. However, 3D printed samples with 20% OG treated TMP had an increase of approximately 190% in tensile strength.	[182]
2018	NC (0.5-3%)	PLA (4032D) and PHBH	Nanocellulose obtained by ultra-sonication of commercial micro cellulose.	No clear evidence of nanocellulose homogeneous dispersion.	Tensile tests of filaments highlighted an improvement of the stiffness (1% NC highest) but a small decrease in tensile strength and failure strain. NC had a detrimental effect on the overall mechanical properties of 3D printed samples (tensile test) because of an increase in porosity.	[186]
2018	MCC - microcrystalline cellulose (1-5%)	PLA (3001D)	Surface treatment of MCC with titanate coupling agent	Surface modification of cellulose decreased the water absorption of the filaments. Increased amount of MCC reduced the crystallinity of PLA.	Mechanical tests not reported.	[187]
2019	NFC (10-40%)	PLA (4033D)	As-received NFC used without further modification (only chopping before mixing with polymer solution)	Up to 50% of NFC used for compression moulding and up to 40% for FDM. Problem with dispersion of NFC was observed. Different printing parameters resulted in different mechanical properties, mainly related to the reduction of inner-bead and inter-bed porosity.	Tensile strength and modulus of 3D printed samples presented similar values of compression moulded composites (up to 30% of NFC), with improvements of up to 45% in strength and 130% in modulus. However, lower strain at break and toughness were observed. The addition of NFC considerably increased the storage modulus up to 100 °C.	[180]
2019	BC – bacterial cellulose (1-2.5%)	PLA (4043D)	The BC was alkali-cooked in a high-shear homogeniser and treated by TEMPO-mediated oxidation (TOBC) according to the method described in [184]	Good dispersion TOBC in PLA was achieved. The addition of TOBC improved the crystallisation rate of PLA, acting as a nucleation agent.	Increase in tensile strength, failure strain, maximum bending strength, and Young's modulus by 9.2%, 202%, 45%, and 49%, respectively, compared to neat PLA by adding 1.5% of TOBC.	[183]
2020	NFC (1-5%)	PLA (4032D)	PEG (used as plasticiser) NFC obtained by enzymatic hydrolysis of MCC (microcrystalline cellulose).	Lack of information regarding the dispersion of NFC in the PLA matrix.	Tensile testing: Increase of 33% in tensile strength and 19% in failure strain (maximum strength and elongation with 2.5% of NFC)	[179]
2020	NFC (1-5%)	PLA (3051D)	Sisal NFC prepared by microgrinding after alkali and bleaching treatments.	The addition of sisal NFC increased the crystallinity of 3D printed PLA by 14%. The NFC also reduced the porosity of the 3D printed objects.	Tensile testing of 3D printed specimen: Increase of tensile strength and Young's modulus by 84% and 63%, respectively by the addition of 1% of sisal NFC in comparison to neat PLA (related to the reduction of porosity and increase in crystallinity).	[188]

(*continued on next page*)

Table 5 (*continued*)

Year	Cellulose source and content (%)	Matrix	Other materials / cellulose treatment	Observation	Mechanical properties / Other findings	Ref.
2020	Nanocellulose (1-5%)	PLA (4032D)	PEG600 (used as plasticiser) The nanocellulose was produced by enzymatic pretreatment and high-pressure microfluidization.	The addition of nanocellulose improved thermal stability and crystallisation rate of PLA, with the best results achieved with 1% of nanocellulose. The addition of PEG600 and nanocellulose reduced the thermal stability of PLA filaments but caused a faster crystallisation rate.	Mechanical tests not reported.	[189]
2020	CNC (5-20%)	PHBH	The CNC crystals were modified by an acetylation process without the use of solvents.	The acetylation process improved the affinity of the CNC with PHBH matrix and formulations with up to 20% of CNC were sucessessfully 3D printed.	The addition of CNC improved the thermal stability and thermo-mechanical properties of the composites. The addition of 20% of CNC increased the storage modulus of the composites by 150%. Samples with CNC presented much faster disintegration degree in a composting process.	[178]

discussed in the publication, this difference between the filaments and 3D printed samples is assumed to be related to the presence of porosity in the filament and the alignment of cellulose fibres during printing. Grafting with LG was not beneficial for the mechanical properties nor water absorption stability [182]

Exploring a different approach for cellulose dispersion, Li et al. 2019 developed a process for TEMPO oxidised bacterial cellulose for PLA reinforcement based on the concept of Pickering emulsion [183]. By combining BC suspension in water and PLA dissolved in dichloromethane (DCM) followed by high-intensity mixing, microparticles containing BC and PLA were obtained, as shown in Fig. 7. The materials were then used to produce FDM filaments by extrusion and 3D printed in a desktop printer. By adding only 1.5% of TEMPO oxidised BC, the authors reported an increase in tensile strength, failure strain, maximum bending strength, and Young's modulus by 9.2%, 202%, 45%, and 49%, respectively. TEMPO (2,2,6,6-tetramethylpiperidine-1-oxyl radical)-mediated oxidation is an effective and important way to obtain nanocellulose fibres with high aspect ratios (>100) without any changes to the original crystallinity with significant amounts of selectively formed C6 carboxylate groups. This oxidation method has been used to improve the dispersion and reactivity of cellulose for surface treatments whenever necessary and widely applied in aerogels and hydrogels formulations [184,185].

4.3. The use of cellulose in inks, gels and thermosets

The use of cellulose has been widely explored for 3D printing of gels/paste formulations. In these methods, compounds are used to produce a gel or ink with special rheological properties suitable to 3D print structures that are submitted to an in situ or a post-printing process by either chemically crosslinking, heat or UV curing, or just drying by heating, freeze-drying, or drying at atmospheric conditions. As previously mentioned, DIW is a commonly used term reported in the literature for syringe printing or liquid/paste deposition modelling; small variations in the printing method are observed depending on the 3D printer used in the experiments. The use of cellulose in other methods, such as DLP, has also been explored to improve the printing quality and mechanical properties UV-curable thermosets [161,190]. The chosen strategy will depend on the target application and formulation properties.

In DIW methods, cellulose has been used in inks, gels, and hydrogels as a responsive element (shape change) [16,20], main component or matrix [19,191–194], reinforcement [17,23,145,191,194–198], and rheology control [17,23,145,195,198] followed by post-printing treatments such as freeze-drying, UV and heat curing, chemical crosslinking, and resin infiltration. In some studies, cellulose is used for multiple purposes, such as structural support, or main component, and also intended as a reinforcement [194]. Moreover, the use of CNC gels as a temporary support material for complex-shaped structures has also been recently explored [199]. These studies envisage new opportunities for the adoption of cellulose-based 3D printed materials in a wide range of emerging applications such as tissue engineering, wound dressing, biomedical devices, soft robotics, composites with tailored architectures and mechanical properties, energy storage, sensors, and flexible electronics. Most relevant developments in this topic have been concentrated in the last 3–5 years.

A comprehensive summary of methodologies, main outcomes, and applications of recent and relevant developments between 2016 and 2020 of cellulose-based formulations used in DIW, or liquid deposition modelling, is given in Table 6. The ink, gel, or hydrogel compositions and printing strategies, including post-printing processes, are depicted. Most studies rely on cellulose as a biocompatible material with reinforcing abilities and as a rheology modifier to develop formulations for 3D printing focused on biomedical applications, with a particular interest in tissue engineering. The controllable porosity of biocompatible cellulose-based structures obtained by 3D printing can be used to allow solvent absorption, cell seeding medium infusion, cell growth, and oxygen permeation, which are important characteristics for tissue engineering applications [192]. As can be seen in the information provided in Table 6, a wide range of strategies and formulations have been explored. Nanocelluloses, e.g., CNC and NFC, are the main sources of cellulose used in all the studies, in which they can be used solely in aqueous suspensions [191,193], or in combination with other natural materials [17,23,194], such as gelatin and alginate, and modified to be used in more complex formulations [191,198].

The rheological properties of nanocellulose suspensions and reinforcing capability of cellulose fibres brought attention for its use to improve the printability of inks based on alginates [19,23,194,200] and gelatines [23,145,195,196]. Jian et al. 2019 used a combination of gelatin and NFC for the development of hydrogels for 3D printing. The addition of 10% of NFC increased 5.75 fold the compressive strength of the printed constructs in comparison with neat gelatin. The addition of NFC also improved the stability of other bioinks made of collagen, fibrin, hyaluronate acid, alginate, chitosan, and agarose [196]. Bacterial cellulose nanofibres (BNCFs) were also used to create hierarchical structures with pores gradient and self-recovery ability in silk fibroin and gelatine hydrogels [145]. The addition of small amounts of BNCF (up to 1.4%) doubled the compressive stress at 30% strain in comparison with

Table 6
Summary of recent advances of cellulose-based formulations for 3D printing using DIW (printing methods and ink/gel formulations descriptions may vary according to the level of details provided in each publication).

Year	Ink/gel formulation	Printing method	Source / use of cellulose	Main outcomes	Possible application	Ref.
2016	Final ink composed of 77.6% deionized water, 0.73% NFC, 9.7% nanoclay, 7.8% monomer (DMAm or NIPAm), 0.097% photoinitiator, 0.23% glucose oxidase, 3.8% glucose.	Syringe printing (DIW) – 200 μm nozzle Printed on glass slides with teflon adhesive. UV-curing after printing.	Unbleached NFC from softwood pulp / Used as anisotropic shrinkage/swelling modifier.	Novel approach developed to calculate and predict hygromorphic transformations. Shape-changing accurately predicted and demonstrated with the formulation based on NFC. The acrylamide was physically crosslinked by the nanoclay particles creating a hydrogel matrix that easily swells in water. Glucose oxidase + glucose successfully used as oxygen scavengers.	Tissue engineering, biomedical devices, soft robotics	[16]
2017	Aqueous-based CNC suspensions (0.5-40 wt%)	Syringe printing (DIW) - 200-410 μm nozzles. Printed onto a hydrophobised glass slide	Eucalyptus pulp CNC obtained by acid hydrolysis / main component	Formulation with 20% was considered the most appropriate (with shear-thinning behaviour). Conditions for the alignment of CNC were quantitatively determined.	Composites with tailored architectures and mechanical properties (programmable reinforcement)	[191]
	CNC-based composites with 10-20% of CNC with HEMA monomer, PUA oligomers, and photoinitiator	Syringe printing (DIW) - 410 μm nozzle. Printed onto a hydrophobised glass slide. Cured using UV source under N_2 environment.	CNC and modified CNC (methacrylic anhydride) / reinforcement	Different mechanical properties achieved (stiff to rubbery) by using different oligomers. CNC modification (vinyl functionality) cause a covalent bond with the polymer. Alignment of CNC during printing results in increases of up to 80% in Young's modulus.		
2017	Aqueous-based CNC suspensions (11.8-30 wt%) and formulations with polyamide-epichlorohydrin (Kymene) addition for crosslinking.	Syringe printing (DIW) – 200-500 μm nozzle. Extruded using an air pressure controller. Printed at 2mm/s. Freeze-dried after printing and heat-cured for crosslinking of formulations with Kymene.	Wood pulp-derived freeze-dried CNC / main component	Aerogels with controlled overall and porous structure using 20% CNC gels were obtained after 3D printing and freeze-drying with densities between 0.127-0.399 g/cm^3 and porosity of 75-92.1%. Crosslinking with Kymene improved the mechanical stability of the aerogels in air and water environments.	Tissue engineering	[192]
2017	Aqueous-based CNC suspensions of 15 wt%	Syringe printing (DIW) – nozzle diameter of 300 μm at a printing pressure of 50 psi and speed of 5mm/s. Structures were freeze-dried after printing.	CNC obtained by oxalic acid hydrolysis of pretreated bleached eucalyptus pulp by disk-milling / main component	The novel CNC production method resulted in high aspect ratio CNC particles. The 15% aqueous CNC suspension presented shear-thinning behaviour and was successfully 3D printed. The structure was maintained after freeze-drying.	Tissue engineering	[193]
2017	Bioink with 0-2.0 % w/v of NFC in a gelatin methacrylamide (GelMA) matrix (5% w/v).	Syringe printing (DIW) – nozzle with an inner diameter of 160 μm, printing pressure of 1-10 psi and speed of 10 mm/s. Crosslinked with (APS/TEMED) after 3D printing.	NFC produced from kraft pulp through mechanical grinding / rheology and reinforcement	The addition of NFC in the bioink formulation ensured its printability. GelMA/NFC composite was successfully crosslinked with APS/TEMED system. The mechanical properties of the 3D printed structures considerably increased with the addition of NFC.	Tissue engineering and other biomedical applications	[195]
2017	NFC and alginate (A) or hyaluronic acid (HA) bioink: 60-80% of NFC (w/w) in relation to A. The NFC/HA ink was prepared with 5 v% of HA in the NFC hydrogel.	Syringe-based 3D bioprinter – printed at room temperature with a nozzle of 300 μm, speed of 10-20 mm/s, and pressure of 2.9-4.3 psi. NFC/A crosslinked with $CaCl_2$ solution and NFC/HA crosslinked with H_2O_2 solution after printing.	NFC produced by enzymatic treatment and mechanical refinement / structural support and reinforcement	Bioink successfully produced and 3D printed for cell encapsulation (human-derived induced pluripotent stem cells and chondrocytes). The structures can be used to support cartilage production.	Tissue engineering – artificial cartilage	[194,201] (2015)

(*continued on next page*)

Table 6 (*continued*)

Year	Ink/gel formulation	Printing method	Source / use of cellulose	Main outcomes	Possible application	Ref.
2017	NFC (2.0-3.3 wt%) and xylan (type of hemicellulose) conjugated with tyramine (XT) with different degrees of substitution.	Syringe-based 3D bioprinter – printed using a conical needle tip (420 μm outlet diameter) at 10 mm/s. Printing pressure adjusted according to each formulation. Crosslinked with H_2O_2 solution after printing.	NFC processed from soft wood pulp by enzymatic pretreatment followed by mechanical grinding and high-pressure homogenisation / reinforcement	Structures successfully printed with reasonable dimensional fidelity. A balanced combination of NFC and XT is necessary for printable and crosslinkable inks. The crosslinking density was tuned by using different degrees of substitution of XT.	Tissue engineering / wound dressing.	[17]
2018	Hydrogel ink composed of CNC suspension, and gelatin (Gel) and sodium alginate (SA) solutions. Final composition (dry) CNC/SA/Gel: 70/20/10.	Syringe-based 3D bioprinter (3D Discovery) – nozzle diameter of 410 μm, speed of 10-80 mm/s. Structures crosslinked with $CaCl_2$ solution after printing.	CNC isolated from pulp of Norway spruce wood by a process developed by [203] / reinforcement and rheology	Scaffolds obtained with gradient porosity within one 3D printed structure. High dimensional fidelity was achieved, with structures with pores sizes between 80–2125 μm (wet condition). Printing parameters drove the print resolution and pore size control. CNC shear-induced alignment observed in the 3D printed structures.	Tissue repair and regeneration	[23]
2018	Ink based on sodium carboxymethyl cellulose (CMC-Na/CMC) as matrix with cellulose pulp (50 v% in dry condition) and montmorillonite clay.	Syringe-based 3D printing using an off-axis direct driven paste extruder. Nozzle of 800 μm. Structures crosslinked by poly acrylic acid, citric acid or self-crosslinking after printing.	Cotton derived pulp fibres / reinforcement and anisotropic swelling/swelling modifier	Dissociation of pulp fibres enabled shear thinning properties to the hydrogel, enabling high fibre loading without clogging during printing. The addition of clay stabilised the printed structures and improved the rheology for printing. Swelling/shrinkage potential influenced by crosslinking strategy.	Not specified	[20]
2019	Ink composed of NFC suspensions with 20% (based on dry content of NFC) of alginate.	Syringe-based 3D printing. Flow speed was 3 mm/s, using a 0.58mm conical nozzle. Structures crosslinked with CaCl after printing	NFC produced from sugarcane bagasse by TEMPO-mediated oxidation pre-treatment followed by homogenisation / main component and reinforcement	TEMPO-oxidised NFC was successfully produced from sugarcane bagasse. The NFC-based inks presented good printability and were found to be cytocompatible. The addition of alginate aided the crosslinking with Ca^{2+} after 3D printing.	Wound dressing devices	[200]
2019	Ink based on nanofibrillated bacterial cellulose (BNFC) (0-1.4%), silk fibroin and gelatine.	3D printed in a bioplotter with polyethylene injection cartridge. Nozzle of 410 μm. Printed at speeds of 3.0-5.2 mm/s. Structures freeze-dried after printing. Some samples were also crosslinked with genipin solution.	BNFC produced by pre-treatment in NaOH solution followed by processing in homogeniser / reinforcement	Scaffolds were printed with hierarchical structure and gradient pores between 10-600 μm. Samples with BNFC had self-recovery ability, and compressive stress at 30% strain doubled in comparison with structures without BNFC. The composites presented excellent biocompatibility and were beneficial for ingrowth of tissue.	Tissue engineering	[145]
2019	Hydrogel composed of 5 w/v% of gelatin and 0-20% of NFC.	3D printed in an extrusion-based printing nozzle controlled by pressure. Nozzle of 210 μm, pressure of 40 psi and speed of 10 mm/s at 10, 15, 20, and 25 °C. Crosslinking solution with different concentrations of genipin after printing.	NFC produced from bleached *Humulus japonicus* stem pulp by high-speed agitation and high-power ultrasonication / reinforcement	The addition of NFC (10%) increased the mechanical strength by 5.75-fold and good shape fidelity with an interconnected porous structure was obtained. The proposed bioink presented good biocompatibility.	Tissue engineering / repair	[196]

(*continued on next page*)

Table 6 (*continued*)

Year	Ink/gel formulation	Printing method	Source / use of cellulose	Main outcomes	Possible application	Ref.
2020	Main gel composed of 20 wt% of CNC and 1 wt% of NFC. Some formulations were infiltrated with HEMA monomer as matrix	Syringe printing (DIW). Nozzle of 410 μm and 27mm long. Printed with pressure of 30-35 psi at 20 °C. Printed structures submitted to freeze-drying or supercritical drying (used for infiltration HEMA monomer as matrix followed by UV-curing).	TEMPO-oxidised NFC produced from bleached softwood pulp and CNC produced from eucalyptus pulp by acid hydrolysis / rheology and reinforcement	Two types of nanocelluloses were applied in the gel formulations. High mechanical properties were achieved by the proposed densification (solvent exchange and monomer infusion) method with up to 27.35 vol% of cellulose. Wet densification explained by the change in the cohesive energy density.	Biomedical and stimuli-reponsive applications	[197]
2020	Gel composed of NFC, alginate, and NaCl and $CaCl_2$ solutions. Solid content of NFC maintained at 19.5 $g.L^{-1}$.	Syringe printing (DIW), piston-driven. Conical 410 μm nozzle printed at 2.9-5.8 psi. Speed adjusted to each formulation. EDOT monomer used for impregnation for in situ polymerisation of PEDOT/TOS as a conducting polymer after printing.	Commerical carboxymethylated NFC / main component (aerogel)	NFC/alginate-based aerogel structures successfully 3D printed and by using freezing, solvent exchange and ambient drying as post-treatments. Large-scale production of these aerogels is envisaged. The addition of salt in the formulation reduced shrinkage by 30%. In situ polymerisation of PEDOT in the aerogel structure resulted in high capacitance (78 F/g).	Energy storage and sensors	[19]
2020	Ink composed of CNC or cin-CNC difunctional with polyurethane acrylate and vinyl cinnamate (50-50 weight ratio). A photoinitiator was also added.	DIW printer using a UV shielded cartridge. Printed with extrusion pressure of 14-43 psi and conical nozzle of 410 μm at 10-15 mm/s. Samples UV-cured after printing. Secondary UV curing was conducted for selective mechanical properties.	CNC obtained from acid hydrolysis of eucalyptus pulp. CNC was also modified (cin-CNC) through grafting with cinnamoyl chloride / rheology and reinforcement.	Structures with tailored mechanical response by selective UV illumination were 3D printed by DIW. Photostiffening was achieved by using biocompatible photocrosslinkable cinnamates. The alignment of modified CNC combined with selective photostiffening created new possibilities for functionally graded materials.	Biomedical prosthetics; sensor, flexible electronics	[198]

DMAm: N,N-dimethylacrylamide; NIPAm: N-isopropylacrylamide; HEMA: 2-Hydroxyethyl methacrylate; PUA: polyurethane-acrylate; APS/TEMED: Ammonium persulfate/ tetramethylethylenediamine
PEDOT/TOS: poly(3,4-ethylenedioxythiophene):tosylate

unreinforced constructs. Similarly, different 3D printed biocompatible structures with outstanding cell growth capabilities using NFC-based inks with alginate or hyaluronic acid were used as support for artificial cartilage production [194,201]. Additionally, a recent study used CNC-based inks with poly(glycerol sebacate) for DIW of multifunctional lattice structures with cell growth capabilities for the treatment of myocardial infarction [202].

Post printing treatments can considerably change and improve the final properties of the printed constructs. The solidification/consolidation phase after 3D printing, especially formulations based on nanocelluloses, is an important step to determine possible applications [143]. By using an innovative way to 3D print cellulose-based inks, Hausmann et al. 2020 introduced wet densification methods to improve the mechanical stability of 3D printed structures. Both CNC and TEMPO-oxidised NFC were used in their formulations. CNC was the main component of the gel for 3D printing while NFC was used as reinforcement. After 3D printing, a series of densification methods were explored: ionic crosslinking and wet infiltration; wet densification and wet infiltration; supercritical drying and infiltration. Monomer solution or dissolved resin were used for the infiltration phase. The investigated processes and obtained materials are presented in Fig. 8. By infiltration and polymerisation of 2-hydroxyethyl methacrylate (HEMA) monomer, they reported Young's modulus and ultimate strength of printed objects in the order of 2 GPa and 22 MPa, respectively, which are superior values than those previously reported for this class of materials. As stated by the authors, this approach opens new opportunities in cellulose-based printed structures with high mechanical properties by using different monomers/polymers for infusion [197].

Using a similar approach, 3D printed NFC-based aerogels were impregnated with a conductive polymer focusing on energy storage applications. 3D printed NFC/alginate aerogels were successfully printed with the addition of salt in the gel before printing. This method enabled the production of stable structures without further crosslinking, with only freezing, solvent exchanging and drying at ambient conditions performed after printing. In situ polymerisation of PEDOT:TOS, poly(3,4-ethylenedioxythiophene):tosylate, a conductive polymer, within the aerogel structure resulted in a material adequate for energy storage with a specific capacitance of 78 F/g [19].

The versatility of cellulose can be observed in other printing methods; cellulose in 3D printing using digital light processing (DLP) has also been recently explored for biomedical applications [161,190]. A resin formulation based on Poly(ethylene glycol) diacrylate (PEGDA) and glycerol 1,3-diglycerolate diacrylate (DiGlyDA) reinforced with CNC (0.2–5%) was used to 3D print complex structures with high superficial quality [161]. The addition of CNC led to improved mechanical properties of the printed objects (up to 151% improvement in Young's modulus but with constant tensile strength) without scarifying the printability of the resin. These promising results are represented in Fig. 9.

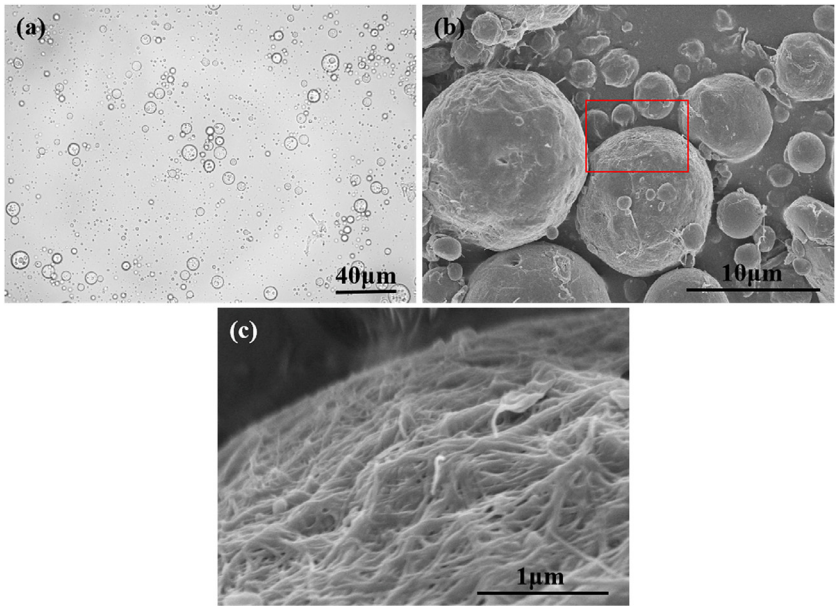

Fig. 7. a) Microscopic image of TEMPO-oxidized BC stabilised in a Pickering emulsion and b), c) SEM image of the PLA/TOBC composite microspheres. Reproduced with permission from Elsevier, license number: 4951510993079 [183].

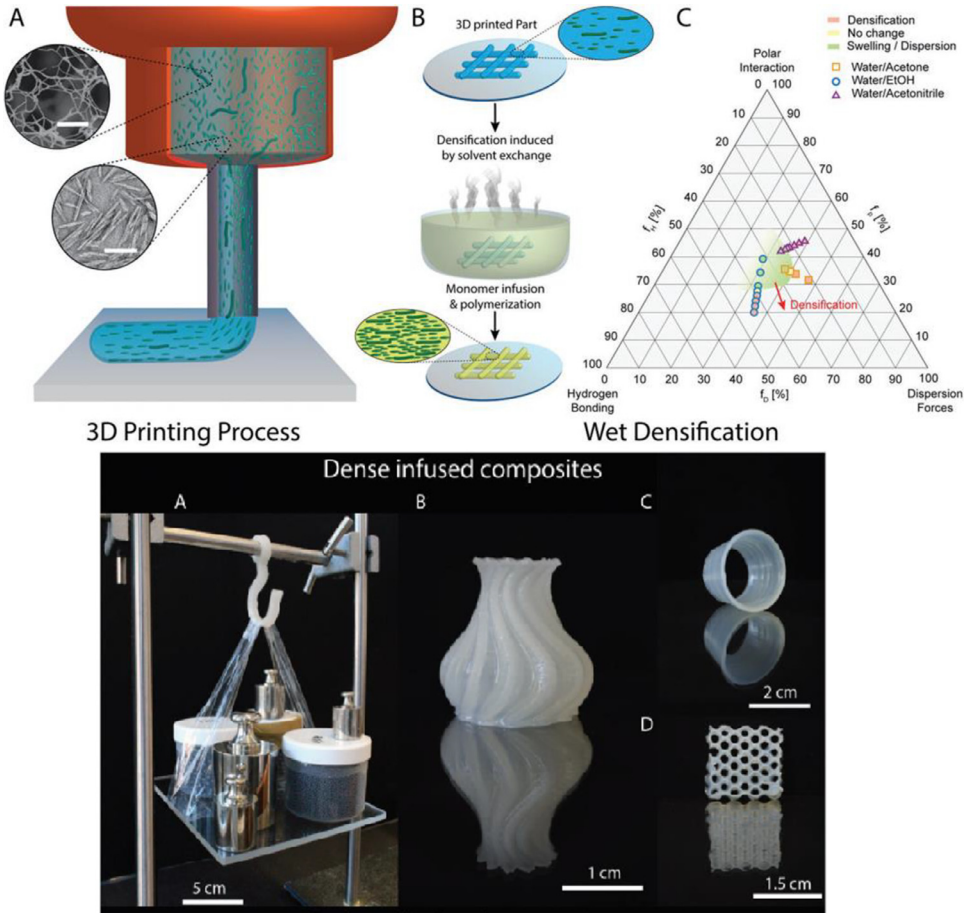

Fig. 8. In the upper image, a schematic representation of the 3D printing process with the alignment of CNCs and CNFs is presented. In B, the wet densification by solvent exchange followed by monomer infusion and polymerisation. In C, a tertiary diagram with the influence of the solvent mixtures solubility parameters, i.e., hydrogen bonding interactions (*f*H), dispersion forces (*f*D), and polar interactions (*f*P), used for solvent-exchange after printing. In the bottom image, examples of structures with high volume fraction of cellulose, 27.35 vol%, produced by different processing routes. Reproduced with permission from John Wiley and Sons, license number: 4951530125186 [197].

4.4. Printability and cellulose alignment

In a concise overview of nanocellulose-based inks for 3D printing, also named as 3D bioprinting, Gatenholm et al. described a methodology for the design of bioink compositions based on requirements for the 3D printing process and application as soft tissues. A troubleshooting flowchart is presented (Fig. 10) to guide future developments in this field [204]. As also identified in other studies, the main requirements for a bioink/gel/hydrogel printability are related to rheological properties during printing and post-printing recovery [205]. Crosslinking is also identified as an essential step to produce structures with mechanical stability [204].

Fig. 11 A shows a methodology to assess the printability of bioinks. First, an initial screening step is suggested to experimentally evaluate

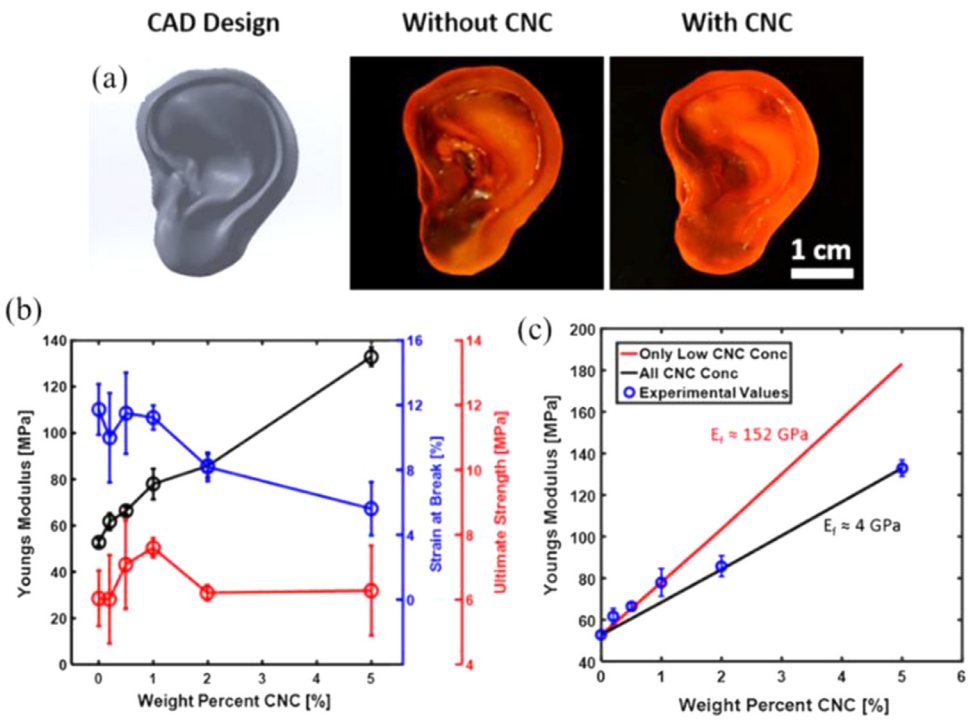

Fig. 9. Results obtained by [161]. a) 3D printed artificial ears by the DLP method according to the CAD design (left) without CNC and with CNC showing that the addition of CNC did not influence on the printing quality. b) The influence of CNC addition on the tensile properties of 3D printed samples. Reproduced with permission from Springer Nature, license number: 4951530415393 [161].

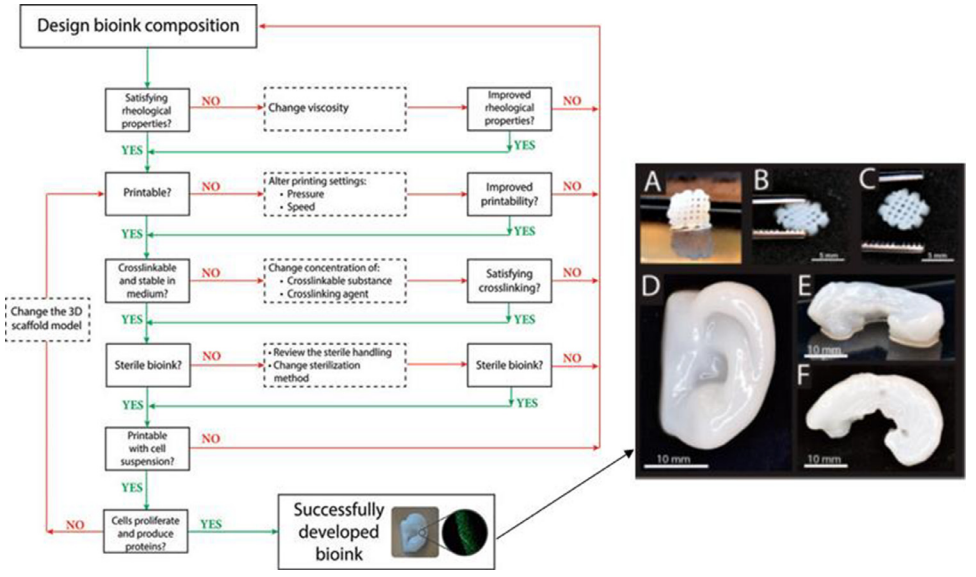

Fig. 10. Troubleshooting flowchart for the development of bioink compositions. Reproduced with permission from Springer Nature, license number: 4951511180779 [204]. Copyright 2016, Springer Nature. Cellulose-based ear successfully printed by DIW followed by chemical crosslinking. Reproduced with permission from [201]. Copyright (2015) American Chemical Society. The initial steps for the development of a bioink also apply for other 3D printing formulations intended for different applications.

fibre (or continuous flow) formation in syringe-based 3D printing and analyse how the layers are stacked. Then, the viscoelastic properties of the suspensions are studied through rheology analyses to identify the shear stress for flow initiation, check if the ink has a shear-thinning behaviour, i.e., if viscosity undergoes a linear decrease with increasing shear rate, and post-printing recovery. After printing, the inks have to present a rapid solid-like response with a sufficient viscosity at zero shear, high storage modulus and yield stress to maintain the construct fidelity/shape [191,205].

As observed in many works, aqueous CNC or NFC-based inks have a shear-thinning behaviour at specific concentrations with no need of rheology modifiers within typical shear rates in DIW printing, which is between 0.01–50 s^{-1} [191]. Size, shape, and surface morphology of the cellulose fibrils were found to have the maximum effect on rheological properties of colloidal suspensions [206]. The effect of different concentrations of CNC in the rheology of dispersions for 3D printing is presented in Fig. 11 B. Dispersions with more than 6 wt% of CNC have an elastic behaviour at low shear rates (elastic shear modulus-G' > viscous modulus-G''), which is suitable for 3D printing. However, high concentrations of CNC may lead to excessively high shear forces that are not achievable in DIW and also lead to plug flow regime, where CNCs are not expected to be aligned. Therefore, the printing parameters and viscoelastic properties of the inks also influence the alignment of cellulose fibres during printing, which is crucial for reinforcement and localised anisotropy purposes, as it will be discussed later in this section [191].

Fibre alignment is a crucial aspect of 3D printing using cellulose-based formulations. Cellulose alignment has been identified as one the most important factors to translate the high mechanical properties of nanocelluloses into bulk materials [207,208] and to amplify cellulose's anisotropic swelling/shrinkage behaviour under different moisture con-

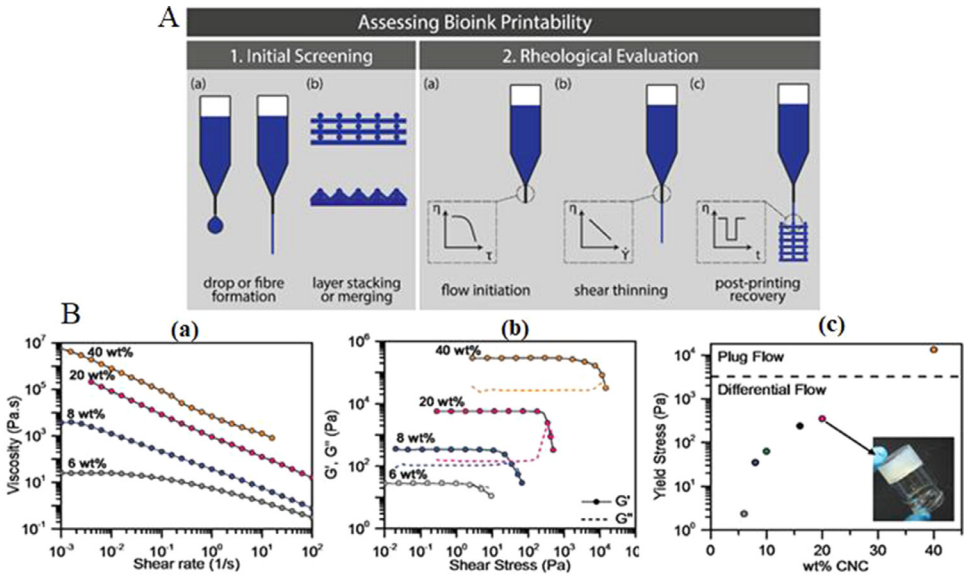

Fig. 11. The rheological characteristics of inks for 3D printing: A) Proposed methodology to assess bioink printability though 1. Initial screening and 2. Rheological assessment to evaluate the a) yield stress for flow initiation (b) shear-thinning behaviour and (c) post-printing recovery [205]. B) Rheological characteristics of dispersions with different concentrations of CNC (6-40 wt%): a) Steady-shear measurement, b) oscillatory rheological, and c) shear yield stress. Reproduced with permission from John Wiley and Sons, license number: 4951521424963 [191].

tent. Therefore, understanding the dynamics of fibre alignment and rheological properties is necessary to design inks and printing methods.

A series of experiments to understand the alignment mechanism during 3D printing by DIW and its correlation with rheology were conducted [191,209]. In general, the alignment of cellulose in composites can be conducted by atomic force microscopy AFM, or more commonly by X-ray diffraction (XRD) techniques (wide angle X-ray scattering (WAXS) or small angle X-ray scaterring (SAXS)). By using AFM it is possible to visually observe the orientation of the CNC particles throughout the 3D printed samples. WAXS, on the other hand, gives more quantitative data since this analysis is related to the crystal orientation of cellulose in a defined direction. By calculating the degree of ordering and Herman's order parameter [210], the quantification of how well cellulose fibres are aligned to a specific direction (printing direction, for example) is estimated. Cross-polarised light used in optical microscopy is a simple method that can also be used to estimate cellulose orientation visually because of the birefringence effect when CNC is used [150,211,212]. By using cross-polarized light, Siqueira et al. compared different printing modes with a solution cast film of CNC based inks for DIW. Those measurements were performed after drying the printed samples (therefore containing 100% CNC). Their findings are presented in Fig. 12 and show the characteristic birefringence effect caused by CNC, with well defined orientated colours in the printed samples.

During printing, the shear stresses arising from the applied pressure are maximal at the nozzle and decrease linearly toward the centre of the nozzle. In order to understand the particle alignment, rheological information is necessary (quantitative analysis), as previously discussed. Cellulose nanocrystals gels are stress-sensitive anisotropic inks, and therefore, the alignment of the particles changes the rheological properties of the fluid as well. There is a complex interplay between the ink rheology, orientation dynamics and local shear rates. Shear stresses during printing must overcome the yield stress of the ink for the alignment of CNCs to occur. In addition, the printing shear stresses must not exceed values that create a plug flow regime, which is dependent on the ink viscosity and nozzle size/geometry [191]

The alignment of CNC during printing was also comprehensively investigated by Hausmann et al. Their experiments showed that the combination of shear and extensional flow in 3D printing nozzles with different geometries is an effective way to tune the orientation of CNCs from aligned to core-shell organisation [209]. An in situ analysis using cross-polarised light integrated into the rheometer setup was used to analyse the alignment and rheology behaviour of CNCs during printing, as presented in Fig. 13. If the printing nozzle induces extensional flow, more substantial alignment is produced, on the contrary of aligned shell around a randomly orientated core, generally produced by pure shear conditions. The CNCs alignment time was found to be linearly depended on the inverse of the shear rate at low shear values whereas, at higher shear values, the interaction between particles (also related to concentration) is more relevant for the alignment dynamics.

4.5. 3D printing of all-cellulose composites and cellulose derivatives

In this section, complementing the information provided in Table 6, recent developments in the use of dissolved cellulose (or partially dissolved) cellulose, also herein named as all-cellulose composites, and cellulose derivatives for additive manufacturing are presented. All-cellulose composites manufactured by conventional methods have been extensively investigated and characterised, presenting outstanding mechanical properties, as presented and discussed in Section 3. However, research on 3D printing of all-cellulose composites (considering the cellulose dissolution approach) has been limited. The main challenges involved in the use of these formulations is on how to dissolve and regenerate (using an anti-solvent) cellulose to obtain high fidelity constructs with reduced/controllable shrinking after regeneration.

The first attempts in 3D printing dissolved cellulose used ionic liquids as a solvent. Markstedt et al. used an ionic liquid, 1-Ethyl-3-methylimidazolium acetate (EmimAc), to dissolve bacterial cellulose and commercial Avicel® (microcrystalline cellulose) at concentrations between 1–4% [213]. Several attempts were conducted to 3D print the obtained gels in a syringe-based 3D printer using water as the anti-solvent (used to regenerate cellulose) during printing either by manually spraying water or by printing in a coagulation gel using agar. The best printing characteristics were obtained by using solutions of 4% of dissolved pulp and agar gel as a regeneration medium. An interconnected porous structure was obtained, but no information regarding mechanical properties is presented [213]. Other ionic liquids, [C4C1Im][OAc] and [C2C1Im][OAc], were also used to dissolve microgranular cellulose with the addition of dimethyl sulfoxide (DMSO) and 1-Butanol as co-solvents for rheology modification [214]. By using 2–5% of dissolved cellulose, different concentrations of DMSO (33–47 wt%) were necessary to make the inks suitable for ink-jet 3D printing. Only small samples in the form of drops were printed and regenerated in deionised water.

Recent works have used more straightforward methods to dissolve cellulose, achieving better mechanical stability of the 3D printed constructs in the wet and regenerated conditions. By using formulations of aqueous N-methylmorpholine N-oxide (NMMO)/cellulose pulp solu-

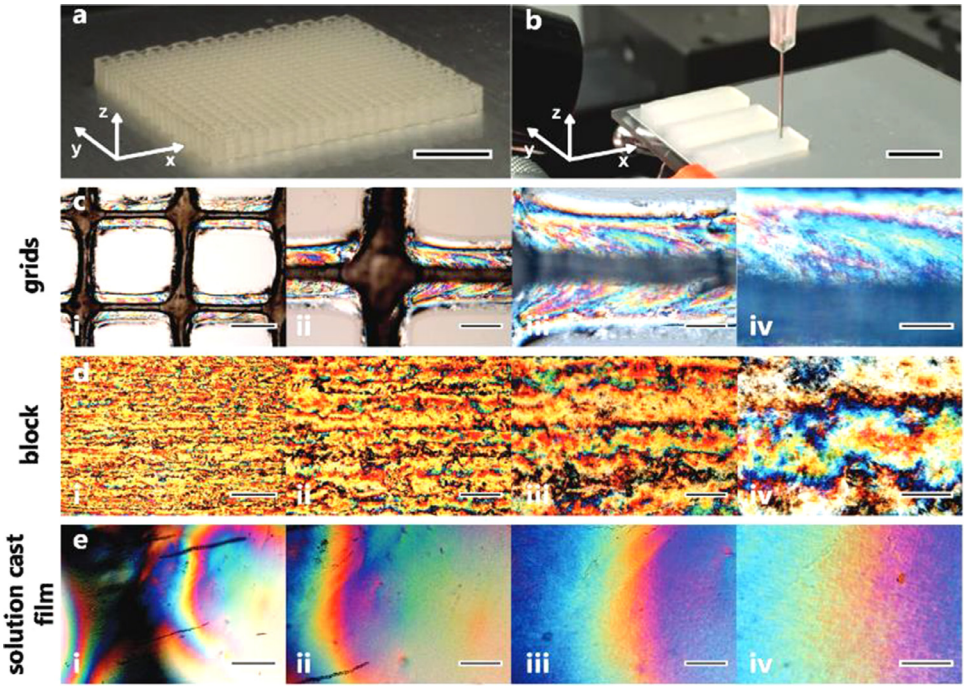

Fig. 12. Qualitative analysis of CNC orientation using cross-polarised light. 3D printed (a) grids and (b) block CNC-based gel (scale bars: 10 mm). Optical microscopy images in cross-polarized light mode of CNC-based structures 3D printed into c) grids and d) top view of block. e) Films obtained by solution-casting. Scale bars: i) 500 µm, ii) 200 µm, iii) 100 µm, and iv) 50 µm. The variation in colour indicated the preferred orientation of CNC fibres. Reproduced with permission from John Wiley and Sons, license number: 4951531043430 [191].

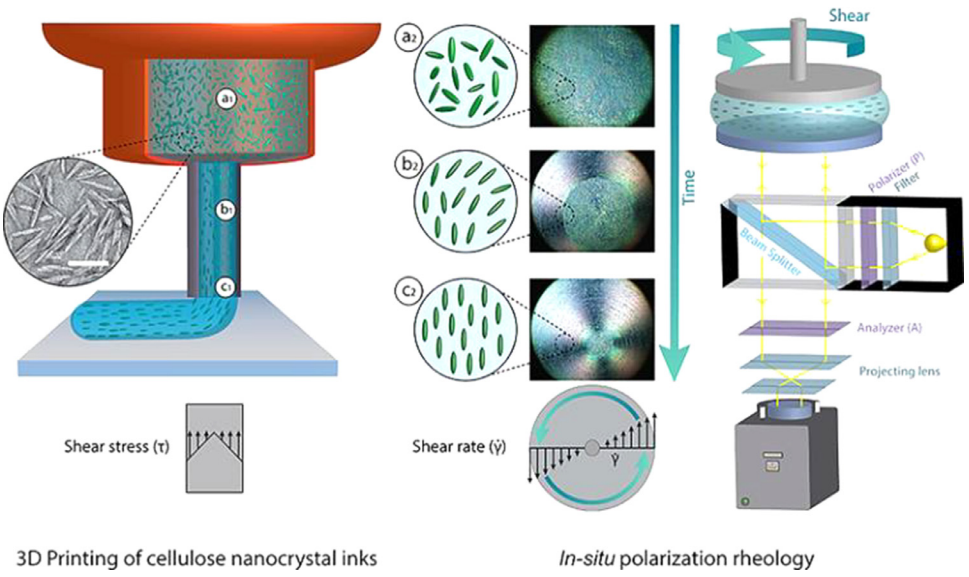

Fig. 13. Alignment of cellulose nanocrystal particles during shearing in DIW (left) and in an in situ polarization rheological setup (right). Left: Schematic of a 3D printing process with (a1) randomly organized cellulose nanocrystals in the cartridge, (b1) shear-induced alignment during extrusion through the nozzle, and (c1) the final oriented extruded segment. Right: Alignment of CNCs under shearing conditions visualized through in situ polarization rheology using a parallel plate geometry. The polarized light imaging system is integrated in the rheometer setup to enable investigation of the effect of shear rate and time on the CNC orientation process (a2, b2, and c2) Reproduced with permission from [209]. Copyright 2018, American Chemical Society.

tions with only 13 wt% of water, Li et al. 3D printed objects at 70 °C by DIW. The extruded gel solidified when exposed to the air, and the generated object was regenerated in deionised water followed by freeze-drying. The 3D printed structure maintained its dimensions and exhibited proper compressive and tensile strengths, even in the gel form [215]. More recently, Jiang et al. obtained constructs with outstanding specific mechanical performance and stability [149]. A NaOH/urea solution was used to dissolve cellulose pulp (as the form of a filter paper) at a low temperature (-12 °C), and the obtained "dope" was 3D printed by DIW. By increasing the cellulose concentration in the NaOH/Urea solution, the ratio of cellulose I/cellulose II increased (determined by X-ray diffraction), which means that some cellulose fibres were only partially dissolved. These partially dissolved fibres worked as reinforcement in the 3D printed structures after regeneration, which considerably improved the mechanical properties. 3D printed and freezed-dried honeycomb structures, like the ones shown in Fig. 14, supported over 15,800 times of its own weight. The authors also explored the use of the obtained materials as a structural thermal insulation material.

With a different strategy, cellulose acetate (CA) dissolved in acetone was used to 3D print dense cellulose constructs (Fig. 15 a) [216]. The main advantage and innovation in this method was the conversion of cellulose acetate into cellulose by deacetylation through immersion in an alcoholic NaOH solution. The authors reported tensile strength and Young's modulus of 55 MPa and 2.5 GPa, respectively, with failure strain of around 12% for the converted 3D printed specimen (Fig. 15 b). These values are higher than those of thermoplastic polymers used for FDM such as PLA, ABS, and Nylon [216]. One important aspected observed in this study is that independently of the printing direction used for the specimens, there was no difference in the tensile properties, i.e., there is no anisotropy, commonly observed in 3D printed samples.

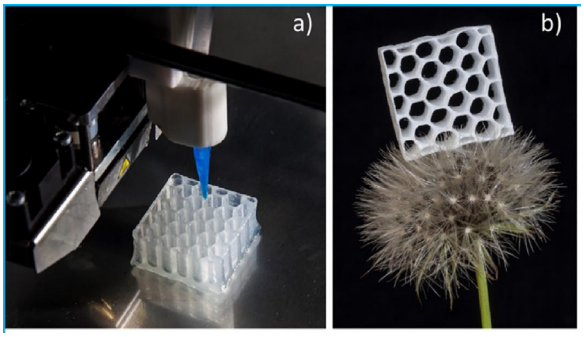

Fig. 14. Images of (a) 3D printing of all-cellulose honeycomb structure; (b) The freeze-dried cellulose honeycomb standing on top of dandelion showing its light-weight Reproduced with permission from Elsevier, license number: 4951540248599 [149].

The use of cellulose derivatives such as hydroxyethylcellulose (HEC) [18], cellulose acetate (CA), acetoxypropyl cellulose (APC) [217], carboxymethylcellulose (CMC) [14,20], and photocurable cellulose acetate butyrate (PC- CAB) [218] have also been explored as promising materials for 3D printing. An example of a novel approach in using cellulose derivatives for 3D printing of structures with controlled stiffness is presented by [18]. Solutions based on HEC present shear-thinning properties and have a pH-dependent gelation time, which allows further adjustments of rheology for 3D printing using different additives. Following a design-to-fabrication workflow approach, inks based on HEC (10 wt%) with microcrystalline cellulose, lignin, and/or citric acid were used to print 2D surfaces with functionally graded properties for programmable deformation through controllable stiffness variations. Similarly, a design-driven approach was used to 3D print by DIW the cellulose derivatives, cellulose acetate (CA) and acetoxypropyl cellulose (APC), onto cellulosic fabrics to produce textiles with controllable properties [217].

Hu et al. explored the use of a cellulose derivative as a photocurable resin for continuous liquid interface production (CLIP), a type of photopolymerization printing method. This method can print an object in minutes by a raising platform that pulls an object created by projecting an image (corresponding to each layer of the object) at a specific light wavelength onto photocurable resins. Cellulose acetate butyrate (CAB) was modified with 2-hydroxyethyl methacrylate (2-HEMA) units to produce a photocurable formulation. The obtained resin was 3D printed by CLIP method and post-treated with UV light to finish the object curing and improve the mechanical properties. The 3D printed material presented high printing fidelity, solvent resistance, and promising mechanical properties, achieving tensile and flexural strengths of 44.7 and 64.5 MPa, respectively [14].

4.6. Cellulose in 4D printing

Design with smart materials for 4D printing includes three essential aspects. Firstly, the use of stimuli-responsive composites which can be blended or incorporated in materials with different properties. The second aspect is the selection of stimuli whose action on the object will allow it to animate correspondingly. Such stimuli include changes in humidity, temperature, magnetic field, and ultraviolet (UV) light. The third aspect of design incorporates the time needed for the stimulation to happen, which results in the property change of the material [219].

Moisture or water-responsive materials have gained popularity in recent years due to their ubiquitous stimulus and a wide range of applications. One of the most significant materials include hydrogels which exhibit special moisture responsivity since their hydrophilic properties allow them to expand up to 200% more than their original volume. Besides, these materials exhibit high printability. However, a drawback with this material is its slower reverse response time implying that a long time is required before the hydrogels dry and shrink back [220].

Several organisms such as leaves and flowers respond to environmental stimuli, leading to dynamic conformations governed by the tissue compositions and anisotropy of the cell walls. By using localised anisotropic swelling/shrinkage behaviour controlled by cellulose alignment, transformations according to external changes may occur. In an emblematic and pioneer work, Gladman et al. reported that a combination of NFC and hydrogel ink resulted in fibre alignment induced by shear forces during printing (the composition of the ink and printing methodology are given in Table 6) [16]. The alignment attained improves transverse swelling, which further allows programming of the 4D-printed structure. The authors used a mathematical model based on the classical Timoshenko model for thermal expansion in bilayers with a metric-driven approach to control the curvature of bilayer structures. Hydrogels' swelling can be regulated through temperature in the ambient environment. By cooling or heating the ambient water, the saturation point can be adjusted, and over swelling can be prevented by employing unique hinge designs. Fig. 16 shows a schematic representation of the main outcomes described in this work, i.e., the effect of 3D processing on the alignment of cellulose fibrils, and the control of shape-changing effect by different designs and cellulose addition [16,221].

By using a similar concept, sodium carboxymethyl cellulose (Na-CMC) was used as a matrix for inks with cellulose pulp, montmorillonite clay, and crosslinking agent (mainly citric acid) to 3D print objects with hygromorphic properties [20]. The high compatibility of the cellulose fibres with the matrix enabled shear thinning behaviour of the formed gel with high fibre loading (50% wt%) without clogging dur-

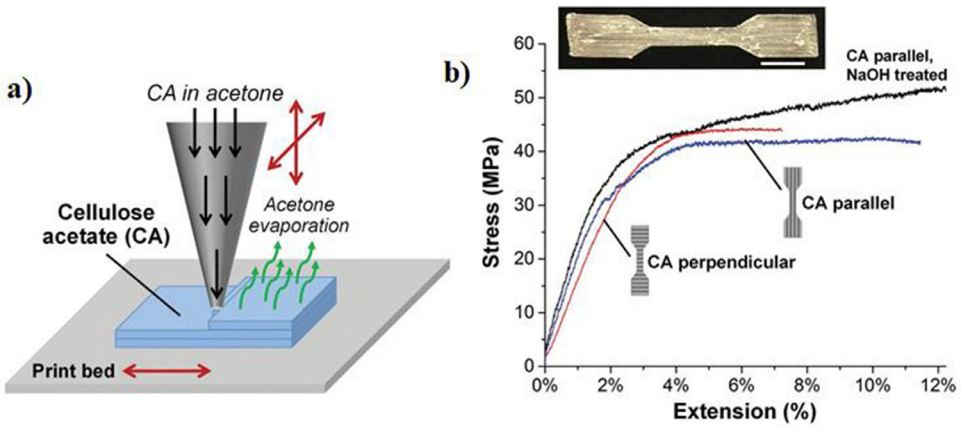

Fig. 15. a) Schematic of cellulose acetate (CA) additive manufacturing process. b) Tensile stress–strain curves of dogbone samples noted (10 points moving average); curves were terminated at point of sudden failure. Inset: image of dogbone part used for tensile testing (scale bar 10 mm). Reproduced with permission from John Wiley and Sons, license number: 4951530614515 [216].

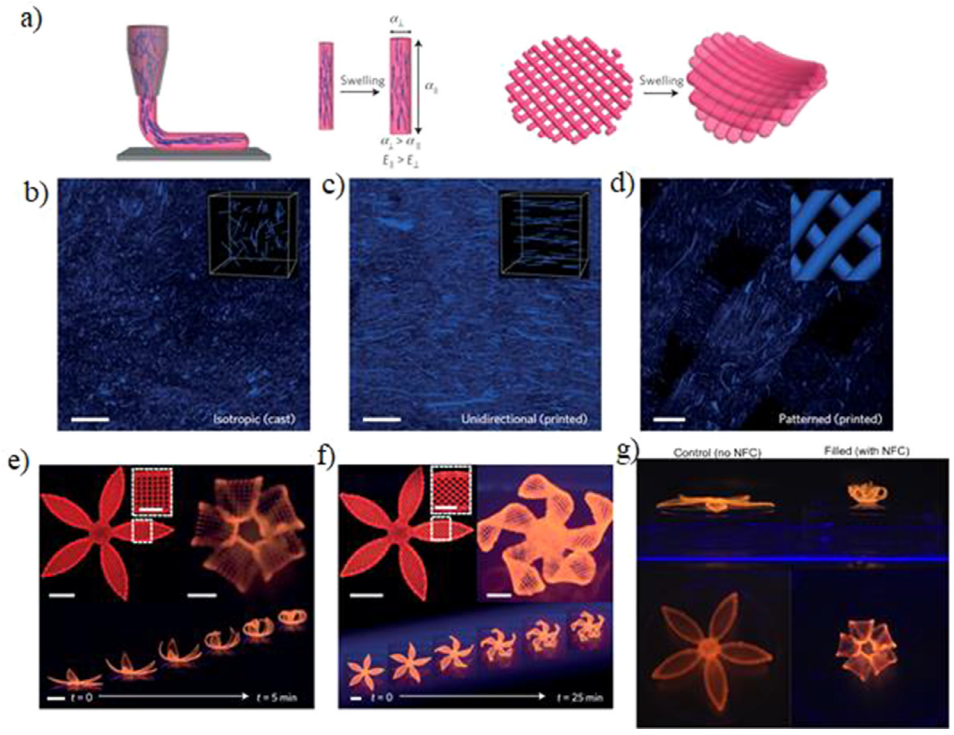

Fig. 16. Biomimetic 3D printing. a) Shear-induced alignment of cellulose fibrils during printing and effect on anisotropic stiffness/swelling strain. b–d) Representation of cellulose fibrils (blue) in isotropic (cast) (b), unidirectional (printed) (c) and patterned (printed) (d) samples (scale bar, 200μm). Generated flower with complex flower morphologies with printed patterns of 90°/0° (e) and 45°/45° (f) [16]. Effect of the addition of NFC (g) with 0 wt% (left), and flower with 0.8 wt% NFC (right). Images obtained after 24 h immersion in water [221]. Reproduced with permission from Springer Nature, license number: 4951530916945 [16].

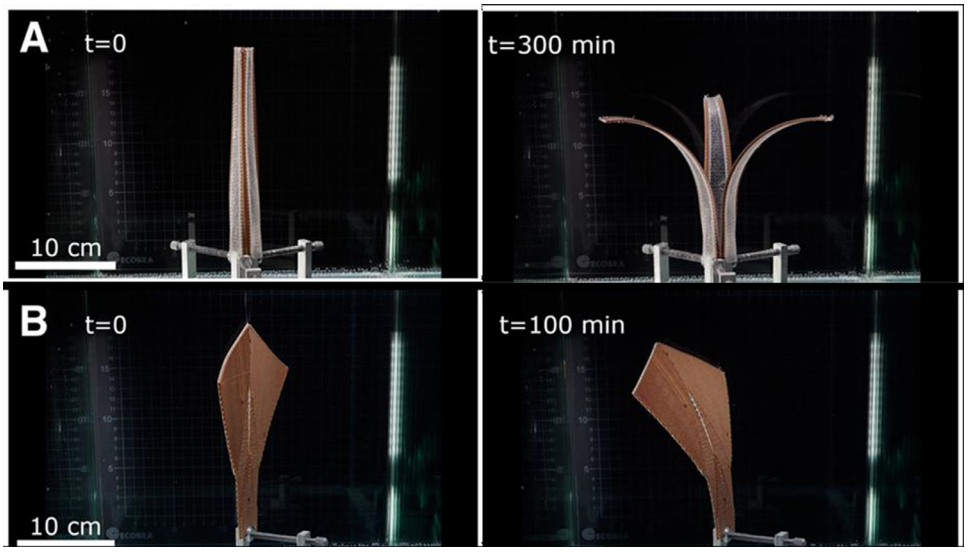

Fig. 17. Moisture responsive behaviour of bilayer 3D printed structures composed of polymer/wood composite and thermoplastics polyurethane layer. Reproduced with permission from Oxford University Press, license number: 4951510827150 [222].

ing printing. Additionally, the addition of clay helped the stabilisation of the construct after printing and improved the rheology of the ink. A shape memory property by hydration/de-hydration cycles was observed, which was described as depended on the crosslinking efficiency and ratio of cellulosic polymers (CMC:HEC).

The use of FDM for 4D printing has been limited to the use of wood filled filaments with hygromorphism [15,33,173]. The use of high cellulose content fibres and nanocellulose for 4D printing is concentrated in DIW method. Fig. 17 shows an example of a 3D printed bilayer structure composed of wood/polymer composite (generally a biopolyester) and a stable layer (TPU) that has a curling effect when exposed to moisture [222]. By increasing the moisture content, the expansion of wood fibres is constrained by the polymer, resulting in a controlled extent and direction of deformation [33]. The main issue with 4D printing hygromorphic wood-based biocomposites is the reduced mechanical properties compared to neat bio-derived polymer filaments.

The use of cellulose has also been explored in different ways for advanced materials. As previously mentioned, in an attempt to create textiles with controllable properties, inks based on the cellulose derivative HEC, microcrystalline cellulose, and other additives were used in combination with cellulosic textiles to create 2D controllable stiffness variations for functionally graded properties, and therefore, programable deformation [18]. This approach can be used for predic Table 2D to 3D transformations by the application of external loads.

Last but not least, the use of cellulose in formulations for 3D printing has opened new opportunities in novel materials orientated to energy storage, sensors, and biomedical applications [19,223]. Sultan et al., 2019 reported a new processing route to 3D print metal-organic frameworks (MOFs), crystalline materials with coordination bond between metal cations and anionic organic linker, based on TEMPO-oxidised NFC (TONFC). The authors reported an in situ growth of MOFs onto TONFCs, favoured by the coordination of Zn^{2+} or Fe^{2+} to the carboxylic groups of

the cellulose fibres. The synthesis and DIW-based printing took place at room temperature using water as a solvent. Additionally, the obtained 3D printed constructs were used for stimuli-responsive (change in pH) release of healing agents, such as curcumin and methylene blue, with potential use in biomedical applications for customised implants (the main advantage of using a 3D printing method) [223]. In another study, the use of NFC was crucial for the development of inks in combination with alginate for 3D printing of aerogel structures [19]. The obtained 3D printed construct presented suitable stability, porosity, and density (23–38 kg/m^3) to be used as a substrate for further functionalisation with other materials. As an example, a conductive polymer was impregnated into the NFC aerogel, resulting in high capacitance values, which can be considered for supercapacitor and sensors applications [19].

5. Summary and outlook

Through this extensive literature review, the unquestionable potential of cellulose as a multifunctional material for a wide range of novel applications is presented. The unique physical, chemical, and mechanical properties of cellulose have been explored for the formulation of new biocomposites, extending its use in additive manufacturing technologies as a binder, matrix, reinforcement, rheology modifier, and stimuli-responsive material.

Although a considerable amount of work has been directed to develop new solutions for 3D printing using cellulose, some challenges still remain. As a reinforcement, cellulose still does not present its true potential considering its intrinsic mechanical properties. To improve the reinforcing performance of cellulose, increasing interfacial bonding and dispersion of cellulose fibres in polymeric matrices are essential. Nevertheless, the technology for 3D printing cellulose-based formulations has been in constant development with new outstanding properties and applications being reported.

Research on 4D printing hygromorphic cellulose composites is still in the initial stages, and further studies are needed to better understand the effects on fibre distribution and orientation on the responsiveness of the materials. Improving mechanical performance along with achieving responsiveness of 4D printed cellulose-based materials is also one of the challenges that need to be addressed.

In general, the versatility of cellulose as a renewable feedstock combined with the freedom of design provided by additive manufacturing is a perfect match for the development of sustainable solutions for advanced applications. In the future, the use of cellulose is envisaged not only for common materials but also in niche commercial applications, where multi-functionality, sustainability, design, and performance, combined, are requested.

Declaration of Competing Interest

The authors declare that they have no known competing financial interests or personal relationships that could have appeared to influence the work reported in this paper.

Acknowledgements

The authors would like to thank the financial support from the Ministry of Business, Innovation and Employment of New Zealand through, National Science Challenge spearhead project “Additive manufacturing and 3D and/or 4D printing of bio-composites’ [grant 2019-S5-CRS] and The University of Waikato for the development of this paper. Special thanks to Dr. John McDonald-Wharry for the rich discussions about 3D printing with cellulose-based materials.

References

[1] HP Fink, P Weigel, HJ Purz, J. Ganster, Structure formation of regenerated cellulose materials from NMMO-solutions, Prog. Polym. Sci. 26 (2001) 1473–1524, doi:10.1016/S0079-6700(01)00025-9.
[2] JP Hinestroza, AN. Netravali, Cellulose Based Composites: New Green Nanomaterials, 9783527327, Wiley-VCH, 2014, doi:10.1002/9783527649440.
[3] D Klemm, B Heublein, HP Fink, A. Bohn, Cellulose: Fascinating biopolymer and sustainable raw material, Angew Chem. Int. Ed. 44 (2005) 3358–3393, doi:10.1002/anie.200460587.
[4] HPS Abdul Khalil, AH Bhat, AF. Ireana Yusra, Green composites from sustainable cellulose nanofibrils: a review, Carbohydr. Polym. 87 (2012) 963–979, doi:10.1016/j.carbpol.2011.08.078.
[5] RJ Moon, A Martini, J Nairn, J Simonsen, J. Youngblood, Cellulose nanomaterials review: structure, properties and nanocomposites, Chem. Soc. Rev. 40 (2011) 3941, doi:10.1039/c0cs00108b.
[6] S Rebouillat, F. Pla, State of the art manufacturing and engineering of nanocellulose: a review of available data and industrial applications, J. Biomater. Nanobiotechnol. 04 (2013) 165–188, doi:10.4236/jbnb.2013.42022.
[7] KJ De France, T Hoare, ED. Cranston, Review of hydrogels and aerogels containing nanocellulose, Chem. Mater. 29 (2017) 4609–4631, doi:10.1021/acs.chemmater.7b00531.
[8] A Dufresne, MN. Belgacem, Cellulose-reinforced composites: from micro-to nanoscale, Polimeros 23 (2013) 277–286, doi:10.4322/polimeros.2010.01.001.
[9] MAS Azizi Samir, F Alloin, A. Dufresne, Review of recent research into cellulosic whiskers, their properties and their application in nanocomposite field, Biomacromolecules 6 (2005) 612–626, doi:10.1021/bm0493685.
[10] J Ganster, HP. Fink, Novel cellulose fibre reinforced thermoplastic materials, Cellulose 13 (2006) 271–280, doi:10.1007/s10570-005-9045-9.
[11] RB Adusumali, M Reifferscheid, H Weber, T Roeder, H Sixta, W. Gindl, Mechanical properties of regenerated cellulose fibres for composites, Macromol. Symp. 244 (2006) 119–125, doi:10.1002/masy.200651211.
[12] H Chai, Y Chang, Y Zhang, Z Chen, Y Zhong, L Zhang, et al., The fabrication of polylactide/cellulose nanocomposites with enhanced crystallization and mechanical properties, Int. J. Biol. Macromol. 155 (2019) 1578–1588, doi:10.1016/j.ijbiomac.2019.11.135.
[13] JM Koo, J Kang, SH Shin, J Jegal, HG Cha, S Choy, et al., Biobased thermoplastic elastomer with seamless 3D-Printability and superior mechanical properties empowered by in-situ polymerization in the presence of nanocellulose, Compos. Sci. Technol. 185 (2020) 107885, doi:10.1016/j.compscitech.2019.107885.
[14] BI Oladapo, EA Oshin, AM. Olawumi, Nanostructural computation of 4D printing carboxymethylcellulose (CMC) composite, Nano-Struct. Nano-Objects 21 (2020) 100423, doi:10.1016/j.nanoso.2020.100423.
[15] D Correa, S Poppinga, MD Mylo, AS Westermeier, B Bruchmann, A Menges, et al., 4D pine scale: biomimetic 4D printed autonomous scale and flap structures capable of multi-phase movement, Philos. Trans. R Soc. A Math. Phys. Eng. Sci. 378 (2020) 20190445, doi:10.1098/rsta.2019.0445.
[16] A Sydney Gladman, EA Matsumoto, RG Nuzzo, L Mahadevan, JA Lewis, Biomimetic 4D printing, Nat Mater 15 (2016) 413–418, doi:10.1038/nmat4544.
[17] K Markstedt, A Escalante, G Toriz, P. Gatenholm, Biomimetic inks based on cellulose nanofibrils and cross-linkable xylans for 3D printing, ACS Appl. Mater. Interfaces 9 (2017) 40878–40886, doi:10.1021/acsami.7b13400.
[18] PAGS Giachini, SS Gupta, W Wang, D Wood, M Yunusa, E Baharlou, et al., Additive manufacturing of cellulose-based materials with continuous, multidirectional stiffness gradients, Sci. Adv. 6 (2020) 1–12, doi:10.1126/sciadv.aay0929.
[19] H Françon, Z Wang, A Marais, K Mystek, A Piper, H Granberg, et al., Ambient-dried, 3D-printable and electrically conducting cellulose nanofiber aerogels by inclusion of functional polymers, Adv. Funct. Mater. (2020), doi:10.1002/adfm.201909383.
[20] MC Mulakkal, RS Trask, VP Ting, AM. Seddon, Responsive cellulose-hydrogel composite ink for 4D printing, Mater. Des. 160 (2018) 108–118, doi:10.1016/j.matdes.2018.09.009.
[21] L Dai, T Cheng, C Duan, W Zhao, W Zhang, X Zou, et al., 3D printing using plant-derived cellulose and its derivatives: a review, Carbohydr. Polym. 203 (2019) 71–86, doi:10.1016/j.carbpol.2018.09.027.
[22] J Li, C Wu, PK Chu, M. Gelinsky, 3D printing of hydrogels: rational design strategies and emerging biomedical applications, Mater. Sci. Eng. R Reports 140 (2020) 100543, doi:10.1016/j.mser.2020.100543.
[23] S Sultan, AP. Mathew, 3D printed scaffolds with gradient porosity based on a cellulose nanocrystal hydrogel, Nanoscale 10 (2018) 4421–4431, doi:10.1039/c7nr08966j.
[24] A Ji, S Zhang, S Bhagia, CG Yoo, AJ. Ragauskas, 3D printing of biomass-derived composites: application and characterization approaches, RSC Adv. 10 (2020) 21698–21723, doi:10.1039/d0ra03620j.
[25] W Gao, Y Zhang, D Ramanujan, K Ramani, Y Chen, CB Williams, et al., The status, challenges, and future of additive manufacturing in engineering, CAD Comput. Aided Des. 69 (2015) 65–89, doi:10.1016/j.cad.2015.04.001.
[26] T Liu, L Liu, C Zeng, Y Liu, J. Leng, 4D printed anisotropic structures with tailored mechanical behaviors and shape memory effects, Compos Sci Technol 186 (2020) 107935, doi:10.1016/j.compscitech.2019.107935.
[27] G N, F M, Smart materials and structures: state of the art and applications, Nano Res. Appl. 04 (2018) 1–5, doi:10.21767/2471-9838.100034.
[28] YC Li, YS Zhang, A Akpek, SR Shin, A. Khademhosseini, 4D bioprinting: the next-generation technology for biofabrication enabled by stimuli-responsive materials, Biofabrication 9 (2017), doi:10.1088/1758-5090/9/1/012001.
[29] T Uchida, H. Onoe, 4D printing of multi-hydrogels using direct ink writing in a supporting viscous liquid, Micromachines 10 (2019), doi:10.3390/mi10070433.
[30] Y Dong, S Wang, Y Ke, L Ding, X Zeng, S Magdassi, et al., 4D printed hydrogels: fabrication, materials, and applications, Adv. Mater. Technol. 5 (2020) 1–19, doi:10.1002/admt.202000034.
[31] T Mohan, A Dobaj Štiglic, M Beaumont, J Konnerth, F Gürer, D Makuc, et al., Generic method for designing self-standing and dual porous 3D bioscaffolds from

cellulosic nanomaterials for tissue engineering applications, ACS Appl. Bio. Mater. 3 (2020) 1197–1209, doi:10.1021/acsabm.9b01099.
[32] W Xu, X Zhang, P Yang, O Långvik, X Wang, Y Zhang, et al., Surface engineered biomimetic inks based on UV cross-linkable wood biopolymers for 3D printing, ACS Appl. Mater. Interfaces 11 (2019) 12389–12400, doi:10.1021/acsami.9b03442.
[33] D Correa, A Papadopoulou, C Guberan, N Jhaveri, S Reichert, A Menges, et al., 3D-printed wood: programming hygroscopic material transformations, 3D Print Addit. Manuf. 2 (2015) 106–116, doi:10.1089/3dp.2015.0022.
[34] E Reyssat, L. Mahadevan, Hygromorphs: from pine cones to biomimetic bilayers, J R Soc. Interface 6 (2009) 951–957, doi:10.1098/rsif.2009.0184.
[35] MA Hubbe, OJ Rojas, LA Lucia, M. Sain, Cellulosic nanocomposites: a review, BioResources 3 (2008) 929–980, doi:10.15376/biores.3.3.929-980.
[36] A Alemdar, M. Sain, Isolation and characterization of nanofibers from agricultural residues - Wheat straw and soy hulls, Bioresour. Technol. 99 (2008) 1664–1671, doi:10.1016/j.biortech.2007.04.029.
[37] W Helbert, Y Nishiyama, T Okano, J. Sugiyama, Molecular imaging of Halocynthia papillosa cellulose, J. Struct. Biol. 124 (1998) 42–50, doi:10.1006/jsbi.1998.4045.
[38] SJ Hanley, JF Revol, L Godbout, DG. Gray, Atomic force microscopy and transmission electron microscopy of cellulose from micrasterias denticulata; evidence for a chiral helical microfibril twist, Cellulose 4 (1997) 209–220, doi:10.1023/A:1018483722417.
[39] M Iguchi, S, B. Yamanaka, Review Bacterial cellulose—a masterpiece of nature's arts, J Mater. Sci. 35 (2000) 261–270, doi:10.1023/A.
[40] R Jonas, LF. Farah, Production and application of microbial cellulose, Polym. Degrad. Stab. (1998), doi:10.1016/S0141-3910(97)00197-3.
[41] J Persson, H Chanzy, J. Sugiyama, Combined infrared and electron diffraction study of the polymorphism of native celluloses, Macromolecules 24 (1991) 2461–2466, doi:10.1021/ma00009a050.
[42] G Mármol, H Savastano, MM Tashima, JL. Provis, Optimization of the $MgOSiO_2$ binding system for fiber-cement production with cellulosic reinforcing elements, Mater. Des. 105 (2016) 251–261, doi:10.1016/j.matdes.2016.05.064.
[43] A Balea, E Fuente, A Blanco, C. Negro, Nanocelluloses: natural-based materials for fiber- reinforced cement composites. a critical review, Polymers (Basel) 11 (2019), doi:10.3390/polym11030518.
[44] Y Yin, L Zhao, X Jiang, H Wang, W. Gao, Poly(lactic acid)-based biocomposites reinforced with modified cellulose nanocrystals, Cellulose 24 (2017) 4773–4784, doi:10.1007/s10570-017-1455-y.
[45] K Oksman, Y Aitomäki, AP Mathew, G Siqueira, Q Zhou, S Butylina, et al., Review of the recent developments in cellulose nanocomposite processing, Compos. Part A Appl. Sci. Manuf. 83 (2016) 2–18, doi:10.1016/j.compositesa.2015.10.041.
[46] R Ajdary, BL Tardy, BD Mattos, L Bai, OJ. Rojas, Plant nanomaterials and inspiration from nature: water interactions and hierarchically structured hydrogels, Adv. Mater. 2001085 (2020), doi:10.1002/adma.202001085.
[47] X Du, Z Zhang, W Liu, Y. Deng, Nanocellulose-based conductive materials and their emerging applications in energy devices - a review, Nano Energy 35 (2017) 299–320, doi:10.1016/j.nanoen.2017.04.001.
[48] Z Shi, GO Phillips, G. Yang, Nanocellulose electroconductive composites, Nanoscale 5 (2013) 3194–3201, doi:10.1039/c3nr00408b.
[49] MM De Souza Lima, R. Borsali, Rodlike cellulose microcrystals: Structure, properties, and applications, Macromol. Rapid Commun. 25 (2004) 771–787, doi:10.1002/marc.200300268.
[50] M. Ioelovich, Characterization of various kinds of nanocellulose, in: I. Ahmad, S. Thomas, A.D.J. Wiley, M. Ioelovich, V. Kinds (Eds.), Handb. Nanocellulose Cellul. Nanocomposites, 2017, pp. 51–100, doi:10.1002/9783527689972.
[51] C Liu, P Luan, Q Li, Z Cheng, P Xiang, D Liu, et al., Biopolymers derived from trees as sustainable multifunctional materials: a review, Adv. Mater. 2001654 (2020) 1–27, doi:10.1002/adma.202001654.
[52] UGK Wegst, MF. Ashby, The mechanical efficiency of natural materials, Philos Mag 84 (2004) 2167–2181, doi:10.1080/14786430410001680935.
[53] AC. O'sullvian, Cellulose: the structure slowly unravels, Cellulose 4 (1997) 173–207.
[54] Y Nishiyama, J Sugiyama, H Chanzy, P. Langan, Crystal structure and hydrogen bonding system in cellulose ib from synchrotron x-ray and neutron fiber diffraction, J. Am. Chem. Soc 125 (2003) 14300–14306, doi:10.1021/ja037055w.
[55] K Leppänen, S Andersson, M Torkkeli, M Knaapila, N Kotelnikova, R. Serimaa, Structure of cellulose and microcrystalline cellulose from various wood species, cotton and flax studied by X-ray scattering, Cellulose 16 (2009) 999–1015, doi:10.1007/s10570-009-9298-9.
[56] D Trache, MH Hussin, CT Hui Chuin, S Sabar, MRN Fazita, OFA Taiwo, et al., Microcrystalline cellulose: isolation, characterization and bio-composites application—a review, Int. J. Biol. Macromol. 93 (2016) 789–804, doi:10.1016/j.ijbiomac.2016.09.056.
[57] X Pan, C Arato, N Gilkes, D Gregg, W Mabee, K Pye, et al., Biorefining of softwoods using ethanol organosolv pulping: preliminary evaluation of process streams for manufacture of fuel-grade ethanol and co-products, Biotechnol. Bioeng. 90 (2005) 473–481, doi:10.1002/bit.20453.
[58] R Jonas, LF. Farah, Production and application of microbial cellulose, Polym. Degrad Stab. 59 (1998) 101–106, doi:10.1016/S0141-3910(97)00197-3.
[59] P Gatenholm, D. Klemm, Bacterial nanocellulose as a renewable material for biomedical applications, MRS Bull. 35 (2010) 208–213, doi:10.1557/mrs2010.653.
[60] V Arantes, IKR Dias, GL Berto, B Pereira, BS Marotti, CFO. Nogueira, The current status of the enzyme-mediated isolation and functionalization of nanocelluloses: production, properties, techno-economics, and opportunities, Cellulose 1 (2020), doi:10.1007/s10570-020-03332-1.
[61] I Siró, D. Plackett, Microfibrillated cellulose and new nanocomposite materials: a review, Cellulose 17 (2010) 459–494, doi:10.1007/s10570-010-9405-y.
[62] T. Lindström, Aspects on nanofibrillated cellulose (NFC) processing, rheology and NFC-film properties, Curr. Opin. Colloid Interface Sci. 29 (2017) 68–75, doi:10.1016/j.cocis.2017.02.005.
[63] MS Reid, M Villalobos, ED. Cranston, Benchmarking cellulose nanocrystals: from the laboratory to industrial production, Langmuir 33 (2017) 1583–1598, doi:10.1021/acs.langmuir.6b03765.
[64] KJ Edgar, CM Buchanan, JS Debenham, PA Rundquist, BD Seiler, MC Shelton, et al., Advances in cellulose ester performance and applicaton, Prog. Polym. Sci. 26 (2001) 1605–1688.
[65] S Zhang, C Chen, C Duan, H Hu, H Li, J Li, et al., Regenerated cellulose by the lyocell process, a brief review of the process and properties, BioResources 13 (2018) 1–16, doi:10.15376/biores.13.2.Zhang.
[66] S Wang, A Lu, L. Zhang, Recent advances in regenerated cellulose materials, Prog Polym Sci 53 (2016) 169–206, doi:10.1016/j.progpolymsci.2015.07.003.
[67] JEM Ballesteros, V dos Santos, G Mármol, M Frías, J. Fiorelli, Potential of the hornification treatment on eucalyptus and pine fibers for fiber-cement applications, Cellulose 24 (2017) 2275–2286, doi:10.1007/s10570-017-1253-6.
[68] V da C Correia, AA da S Curvelo, K Marabezi, AEF de S Almeida, H. Savastano Jr., Bamboo cellulosic pulp produced by the ethanol/water process for reinforcement applications, Cienc Florest 25 (2015) 127–135, doi:10.1590/10.1590/1980-509820152505127.
[69] F Li, E Mascheroni, L. Piergiovanni, The potential of nanocellulose in the packaging field: a review, Packag Technol. Sci. 28 (2015) 475–508, doi:10.1002/pts.2121.
[70] FV. Ferreira, IF Pinheiro, RF Gouveia, GP Thim, LMF. Lona, Functionalized cellulose nanocrystals as reinforcement in biodegradable polymer nanocomposites, Polym. Compos. 39 (2018) E9–29, doi:10.1002/pc.24583.
[71] AJ Sayyed, NA Deshmukh, DV. Pinjari, A critical review of manufacturing processes used in regenerated cellulosic fibres: viscose, cellulose acetate, cuprammonium, LiCl/DMAc, ionic liquids, and NMMO based lyocell, Cellulose 26 (2019) 2913–2940, doi:10.1007/s10570-019-02318-y.
[72] N Graupner, G Ziegmann, J. Müssig, Composite models for compression moulded long regenerated cellulose fibre-reinforced brittle polylactide (PLA), Compos. Sci. Technol. 149 (2017) 55–63, doi:10.1016/j.compscitech.2017.05.028.
[73] N Graupner, AS Herrmann, J. Müssig, Natural and man-made cellulose fibre-reinforced poly(lactic acid) (PLA) composites: an overview about mechanical characteristics and application areas, Compos. Part A Appl. Sci. Manuf. 40 (2009) 810–821, doi:10.1016/j.compositesa.2009.04.003.
[74] YRJ. Eichhorn, The young's modulus of a microcrystalline cellulose, Cellulose 8 (2001) 197–207, doi:10.1023/A:1013181804540.
[75] L Mott, L Groom, S. Shaler, Mechanical properties of individual southern pine fibers. Part II. Comparison of earlywood and latewood fibers with respect to tree height and juvenility, Wood Fiber Sci. 34 (2002) 221–237.
[76] R Rusli, SJ. Eichhorn, Determination of the stiffness of cellulose nanowhiskers and the fiber-matrix interface in a nanocomposite using Raman spectroscopy, Appl. Phys. Lett. 93 (2008), doi:10.1063/1.2963491.
[77] RR Lahiji, X Xu, R Reifenberger, A Raman, A Rudie, RJ Moon, Atomic force microscopy characterization of cellulose nanocrystals, Langmuir 26 (2010) 4480–4488, doi:10.1021/la903111j.
[78] G Guhados, W Wan, JL. Hutter, Measurement of the elastic modulus of single bacterial cellulose fibers using atomic force microscopy, Langmuir 21 (2005) 6642–6646, doi:10.1021/la0504311.
[79] YC Hsieh, H Yano, M Nogi, SJ. Eichhorn, An estimation of the Young's modulus of bacterial cellulose filaments, Cellulose 15 (2008) 507–513, doi:10.1007/s10570-008-9206-8.
[80] M Matsuo, C Sawatari, Y Iwai, F. Ozaki, Effect of orientation distribution and crystallinity on the measurement by x-ray diffraction of the crystal lattice moduli of cellulose i and ii, Macromolecules 23 (1990) 3266–3275, doi:10.1021/ma00215a012.
[81] I Diddens, B Murphy, M Krisch, M. Müller, Anisotropic elastic properties of cellulose measured using inelastic X-ray scattering, Macromolecules 41 (2008) 9755–9759, doi:10.1021/ma801796u.
[82] K Tashiro, M. Kobayashi, Theoretical evaluation of three-dimensional elastic constants of native and regenerated celluloses: role of hydrogen bonds, Polymer (Guildf) 32 (1991) 1516–1526, doi:10.1016/0032-3861(91)90435-L.
[83] SJ Eichhorn, GR. Davies, Modelling the crystalline deformation of native and regenerated cellulose, Cellulose 13 (2006) 291–307, doi:10.1007/s10570-006-9046-3.
[84] S Reiling, J. Brickmann, Theoretical investigations on the structure and physical properties of cellulose, Macromol Theory Simulations 4 (1995) 725–743, doi:10.1002/mats.1995.040040409.
[85] SJ Eichhorn, RJ Young, GR. Davies, Modeling crystal and molecular deformation in regenerated cellulose fibers, Biomacromolecules 6 (2005) 507–513, doi:10.1021/bm049409x.
[86] SJ Eichhorn, J Sirichaisit, RJ. Young, Deformation mechanisms in cellulose fibres, paper and wood, J. Mater. Sci. 36 (2001) 3129–3135, doi:10.1023/A:1017969916020.
[87] Northolt MG, den Decker P, Picken SJ, Baltussen JJM, Schlatmann R. The tensile strength of polymer fibres. Polym. Inorg. Fibers, Berlin/Heidelberg: Springer-Verlag; n.d., p. 1–108. https://doi.org/10.1007/b104207.
[88] KL Pickering, MGA Efendy, TM. Le, A review of recent developments in natural fibre composites and their mechanical performance, Compos. Part A Appl. Sci. Manuf. 83 (2016) 98–112, doi:10.1016/j.compositesa.2015.08.038.
[89] DU. Shah, Developing plant fibre composites for structural applications by optimising composite parameters: a critical review, J. Mater. Sci. 48 (2013) 6083–6107, doi:10.1007/s10853-013-7458-7.
[90] MDH Beg, KL. Pickering, Reprocessing of wood fibre reinforced polypropylene composites. Part I: Effects on physical and mechanical properties, Compos. Part A Appl. Sci. Manuf 39 (2008) 1091–1100, doi:10.1016/j.compositesa.2008.04.013.

[91] MDH Beg, KL. Pickering, Reprocessing of wood fibre reinforced polypropylene composites. Part II: hygrothermal ageing and its effects, Compos. Part A Appl. Sci. Manuf. 39 (2008) 1565–1571, doi:10.1016/j.compositesa.2008.06.002.
[92] A Abdulkhani, J Hosseinzadeh, A Ashori, S Dadashi, Z. Takzare, Preparation and characterization of modified cellulose nanofibers reinforced polylactic acid nanocomposite, Polym. Test 35 (2014) 73–79, doi:10.1016/j.polymertesting.2014.03.002.
[93] JW Rhim, HM Park, CS. Ha, Bio-nanocomposites for food packaging applications, Prog. Polym. Sci. 38 (2013) 1629–1652, doi:10.1016/j.progpolymsci.2013.05.008.
[94] SS Nair, C Dartiailh, DB Levin, N. Yan, Highly toughened and transparent biobased epoxy composites reinforced with cellulose nanofibrils, Polymers (Basel) 11 (2019), doi:10.3390/polym11040612.
[95] L Yue, F Liu, S Mekala, A Patel, RA Gross, Zloczower Manas, High performance biobased epoxy nanocomposite reinforced with a bacterial cellulose nanofiber network, ACS Sustain. Chem. Eng. 7 (2019) 5986–5992, doi:10.1021/acssuschemeng.8b06073.
[96] G Chen, X Chen, F Wu, J. Chen, Advanced industrial and engineering polymer research polyhydroxyalkanoates (PHA) toward cost competitiveness and functionality, Adv. Ind. Eng. Polym. Res. 3 (2020) 1–7, doi:10.1016/j.aiepr.2019.11.001.
[97] KL. Pickering, Properties and Performance of Natural Fibre Composites, Woodhead Publishing; Maney Publishing; CRC Press, Cambridge, England: [England?]: Boca Raton, FL, 2008.
[98] SK Ramamoorthy, M Skrifvars, A. Persson, A review of natural fibers used in biocomposites: Plant, animal and regenerated cellulose fibers, Polym. Rev. 55 (2015) 107–162, doi:10.1080/15583724.2014.971124.
[99] X Yang, SK Biswas, J Han, S Tanpichai, MC Li, C Chen, et al., Surface and interface engineering for nanocellulosic advanced materials, Adv. Mater. (2020), doi:10.1002/adma.202002264.
[100] Eichhorn SJ, Dufresne A, Aranguren M, Marcovich NE, Capadona JR, Rowan SJ, et al. Review: Current international research into cellulose nanofibres and nanocomposites. vol. 45. 2010. https://doi.org/10.1007/s10853-009-3874-0.
[101] X Qiu, S. Hu, Smart" materials based on cellulose: a review of the preparations, properties, and applications, Materials (Basel) 6 (2013) 738–781, doi:10.3390/ma6030738.
[102] C Wan, Y Jiao, S Wei, L Zhang, Y Wu, J. Li, Functional nanocomposites from sustainable regenerated cellulose aerogels: a review, Chem. Eng. J. 359 (2019) 459–475, doi:10.1016/j.cej.2018.11.115.
[103] M Mariano, N El Kissi, A. Dufresne, Cellulose nanocrystals and related nanocomposites: Review of some properties and challenges, J. Polym. Sci. Part B Polym. Phys. 52 (2014) 791–806, doi:10.1002/polb.23490.
[104] L Xiao, Y Mai, F He, L Yu, L Zhang, H Tang, et al., Bio-based green composites with high performance from poly(lactic acid) and surface-modified microcrystalline cellulose, J. Mater. Chem. 22 (2012) 15732–15739, doi:10.1039/c2jm32373g.
[105] B Baghaei, M. Skrifvars, Characterisation of polylactic acid biocomposites made from prepregs composed of woven polylactic acid/hemp-Lyocell hybrid yarn fabrics, Compos. Part A Appl. Sci. Manuf. 81 (2016) 139–144, doi:10.1016/j.compositesa.2015.10.042.
[106] SS Nair, H Chen, Y Peng, Y Huang, N. Yan, Polylactic acid biocomposites reinforced with nanocellulose fibrils with high lignin content for improved mechanical, thermal, and barrier properties, ACS Sustain. Chem. Eng. 6 (2018) 10058–10068, doi:10.1021/acssuschemeng.8b01405.
[107] JK Muiruri, S Liu, WS Teo, J Kong, C. He, Highly biodegradable and tough polylactic acid-cellulose nanocrystal composite, ACS Sustain. Chem. Eng. 5 (2017) 3929–3937, doi:10.1021/acssuschemeng.6b03123.
[108] Y Yin, L Zhao, X Jiang, H Wang, W. Gao, Cellulose nanocrystals modified with a triazine derivative and their reinforcement of poly(lactic acid)-based bionanocomposites, Cellulose 25 (2018) 2965–2976, doi:10.1007/s10570-018-1741-3.
[109] Y Yin, LA Lucia, L Pal, X Jiang, MA. Hubbe, Lipase-catalyzed laurate esterification of cellulose nanocrystals and their use as reinforcement in PLA composites, Cellulose 27 (2020) 6263–6273, doi:10.1007/s10570-020-03225-3.
[110] M Gonzalo, C Gauss, R. Fangueiro, Potential of cellulose microfibers for PHA and PLA biopolymers reinforcement, Molecules 25 (2020) 4653, doi:10.3390/molecules25204653.
[111] S Geng, D Wloch, N Herrera, K. Oksman, Large-scale manufacturing of ultra-strong, strain-responsive poly(lactic acid)-based nanocomposites reinforced with cellulose nanocrystals, Compos. Sci. Technol. 194 (2020) 108144, doi:10.1016/j.compscitech.2020.108144.
[112] MS Huda, AK Mohanty, LT Drzal, E Schut, M. Misra, Green" composites from recycled cellulose and poly(lactic acid): Physico-mechanical and morphological properties evaluation, J. Mater. Sci. 40 (2005) 4221–4229, doi:10.1007/s10853-005-1998-4.
[113] J Ganster, HP Fink, M. Pinnow, High-tenacity man-made cellulose fibre reinforced thermoplastics - Injection moulding compounds with polypropylene and alternative matrices, Compos. Part A Appl. Sci. Manuf. 37 (2006) 1796–1804, doi:10.1016/j.compositesa.2005.09.005.
[114] B Bax, J. Müssig, Impact and tensile properties of PLA/Cordenka and PLA/flax composites, Compos. Sci. Technol. 68 (2008) 1601–1607, doi:10.1016/j.compscitech.2008.01.004.
[115] AN Nakagaito, A Fujimura, T Sakai, Y Hama, H. Yano, Production of microfibrillated cellulose (MFC)-reinforced polylactic acid (PLA) nanocomposites from sheets obtained by a papermaking-like process, Compos. Sci. Technol. 69 (2009) 1293–1297, doi:10.1016/j.compscitech.2009.03.004.
[116] N. Graupner, Improvement of the mechanical properties of biodegradable hemp fiber reinforced poly(lactic acid) (PLA) composites by the admixture of man-made cellulose fibers, J. Compos. Mater. 43 (2009) 689–702, doi:10.1177/0021998308100688.
[117] N Graupner, J. Müssig, A comparison of the mechanical characteristics of kenaf and lyocell fibre reinforced poly(lactic acid) (PLA) and poly(3-hydroxybutyrate) (PHB) composites, Compos. Part A Appl. Sci. Manuf. 42 (2011) 2010–2019, doi:10.1016/j.compositesa.2011.09.007.
[118] S Tanpichai, WW Sampson, SJ. Eichhorn, Stress-transfer in microfibrillated cellulose reinforced poly(lactic acid) composites using Raman spectroscopy, Compos. Part A Appl. Sci. Manuf. 43 (2012) 1145–1152, doi:10.1016/j.compositesa.2012.02.006.
[119] M Feldmann, AK. Bledzki, Bio-based polyamides reinforced with cellulosic fibres - processing and properties, Compos. Sci. Technol. 100 (2014) 113–120, doi:10.1016/j.compscitech.2014.06.008.
[120] N El Miri, K Abdelouahdi, M Zahouily, A Fihri, A Barakat, A Solhy, et al., Bio-nanocomposite films based on cellulose nanocrystals filled polyvinyl alcohol/chitosan polymer blend, J. Appl. Polym. Sci. 132 (2015) 1–13, doi:10.1002/app.42004.
[121] KC Seavey, I Ghosh, RM Davis, WG. Glasser, Continuous cellulose fiber-reinforced cellulose ester composites I. Manufacturing options, Cellulose 8 (2001) 149–159, doi:10.1023/A:1016713131851.
[122] W Gindl, J. Keckes, All-cellulose nanocomposite, Polymer (Guildf) 46 (2005) 10221–10225, doi:10.1016/j.polymer.2005.08.040.
[123] X Zhang, Y. Zhang, Reinforcement effect of poly(butylene succinate) (PBS)-grafted cellulose nanocrystal on toughened PBS/polylactic acid blends, Carbohydr. Polym. 140 (2016) 374–382, doi:10.1016/j.carbpol.2015.12.073.
[124] H Ma, B Zhou, HS Li, YQ Li, SY. Ou, Green composite films composed of nanocrystalline cellulose and a cellulose matrix regenerated from functionalized ionic liquid solution, Carbohydr. Polym. 84 (2011) 383–389, doi:10.1016/j.carbpol.2010.11.050.
[125] JW Dormanns, J Schuermann, J Müssig, BJC Duchemin, MP. Staiger, Solvent infusion processing of all-cellulose composite laminates using an aqueous NaOH/urea solvent system, Compos. Part A Appl. Sci. Manuf. 82 (2016) 130–140, doi:10.1016/j.compositesa.2015.12.002.
[126] N Soykeabkaew, T Nishino, T. Peijs, All-cellulose composites of regenerated cellulose fibres by surface selective dissolution, Compos. Part A Appl. Sci. Manuf 40 (2009) 321–328, doi:10.1016/j.compositesa.2008.10.021.
[127] N Soykeabkaew, C Sian, S Gea, T Nishino, T. Peijs, All-cellulose nanocomposites by surface selective dissolution of bacterial cellulose, Cellulose 16 (2009) 435–444, doi:10.1007/s10570-009-9285-1.
[128] F Dong, M Yan, C Jin, S. Li, Characterization of type-II acetylated cellulose nanocrystals with various degree of substitution and its compatibility in PLA films, Polymers (Basel) 9 (2017) 1–14, doi:10.3390/polym9080346.
[129] W Li, X He, Y Zuo, S Wang, Y. Wu, Study on the compatible interface of bamboo fiber/polylactic acid composites by in-situ solid phase grafting, Int. J. Biol. Macromol. 141 (2019) 325–332, doi:10.1016/j.ijbiomac.2019.09.005.
[130] N Esmaeili, FO Bakare, M Skrifvars, S Javanshir Afshar, D Åkesson, Mechanical properties for bio-based thermoset composites made from lactic acid, glycerol and viscose fibers, Cellulose 22 (2015) 603–613, doi:10.1007/s10570-014-0500-3.
[131] T Chen, W. Liu, Highly unsaturated microcrystalline cellulose and its cross-linked soybean-oil-based thermoset composites, ACS Sustain. Chem. Eng. 7 (2019) 1796–1805, doi:10.1021/acssuschemeng.8b05968.
[132] T Huber, J Müssig, O Curnow, S Pang, S Bickerton, MP. Staiger, A critical review of all-cellulose composites, J. Mater. Sci. 47 (2012) 1171–1186, doi:10.1007/s10853-011-5774-3.
[133] N Soykeabkaew, N Arimoto, T Nishino, T. Peijs, All-cellulose composites by surface selective dissolution of aligned ligno-cellulosic fibres, Compos. Sci. Technol. 68 (2008) 2201–2207, doi:10.1016/j.compscitech.2008.03.023.
[134] S Kalka, T Huber, J Steinberg, K Baronian, J Müssig, MP. Staiger, Biodegradability of all-cellulose composite laminates, Compos. Part A Appl. Sci. Manuf. 59 (2014) 37–44, doi:10.1016/j.compositesa.2013.12.012.
[135] A van Wijk, I. van Wijk, 3D Printing with Biomaterials: Towards a Sustainable and Circular Economy, 2015, doi:10.3233/978-1-61499-486-2-i.
[136] S Bose, D Ke, H Sahasrabudhe, A. Bandyopadhyay, Additive manufacturing of biomaterials, Prog. Mater. Sci. 93 (2018) 45–111, doi:10.1016/j.pmatsci.2017.08.003.
[137] S, I Adiloğlu, C Yu, R Chen, JJ Li, JJ Li, et al., We are IntechOpen, the world ' s leading publisher of Open Access books Built by scientists, for scientists TOP 1 %, Intech i (2012) 13, doi:10.1016/j.colsurfa.2011.12.014.
[138] D. Chhabra, Comparison and analysis of different 3D printing techniques, Int. J. Latest Trends Eng Technol 8 (2017) 264–272, doi:10.21172/1.841.44.
[139] D Stoof, K. Pickering, Sustainable composite fused deposition modelling filament using recycled pre-consumer polypropylene, Compos. Part B Eng. 135 (2018) 110–118, doi:10.1016/j.compositesb.2017.10.005.
[140] E Gkartzou, EP Koumoulos, CA. Charitidis, Production and 3D printing processing of bio-based thermoplastic filament, Manuf. Rev. 4 (2017), doi:10.1051/mfreview/2016020.
[141] H Françon, Z Wang, A Marais, K Mystek, A Piper, H Granberg, et al., Ambient-dried, 3D-printable and electrically conducting cellulose nanofiber aerogels by inclusion of functional polymers, Adv. Funct. Mater. 30 (2020), doi:10.1002/adfm.201909383.
[142] VCF Li, A Mulyadi, CK Dunn, Y Deng, HJ. Qi, Direct ink write 3D printed cellulose nanofiber aerogel structures with highly deformable, shape recoverable, and functionalizable properties, ACS Sustain. Chem. Eng. 6 (2018) 2011–2022, doi:10.1021/acssuschemeng.7b03439.
[143] KMO Håkansson, IC Henriksson, C de la Peña Vázquez, V Kuzmenko, K Markstedt, P Enoksson, et al., Solidification of 3D printed nanofibril hydrogels into functional 3D cellulose structures, Adv. Mater. Technol. 1 (2016) 1–9, doi:10.1002/admt.201600096.

[144] X Zhang, M Morits, C Jonkergouw, A Ora, JJ Valle-Delgado, M Farooq, et al., Three-dimensional printed cell culture model based on spherical colloidal lignin particles and cellulose nanofibril-alginate hydrogel, Biomacromolecules 21 (2020) 1875–1885, doi:10.1021/acs.biomac.9b01745.
[145] L Huang, X Du, S Fan, G Yang, H Shao, D Li, et al., Bacterial cellulose nanofibers promote stress and fidelity of 3D-printed silk based hydrogel scaffold with hierarchical pores, Carbohydr. Polym. 221 (2019) 146–156, doi:10.1016/j.carbpol.2019.05.080.
[146] C Feng, J-P Zhou, X-D Xu, Y-N Jiang, H-C Shi, G-Q. Zhao, Research on 3D bio-printing molding technology of tissue engineering scaffold by nanocellulose/gelatin hydrogel composite, BioResources 14 (2019) 9244–9257.
[147] S Sultan, G Siqueira, T Zimmermann, AP. Mathew, 3D printing of nano-cellulosic biomaterials for medical applications, Curr. Opin. Biomed. Eng. 2 (2017) 29–34, doi:10.1016/j.cobme.2017.06.002.
[148] Q Wang, J Sun, Q Yao, C Ji, J Liu, Q. Zhu, 3D printing with cellulose materials, Cellulose 25 (2018) 4275–4301, doi:10.1007/s10570-018-1888-y.
[149] J Jiang, H Oguzlu, F. Jiang, 3D printing of lightweight, super-strong yet flexible all-cellulose structure, Chem. Eng. J. 405 (2021) 126668, doi:10.1016/j.cej.2020.126668.
[150] K De France, Z Zeng, T Wu, G. Nyström, Functional materials from nanocellulose: utilizing structure–property relationships in bottom-up fabrication, Adv. Mater. 2000657 (2020), doi:10.1002/adma.202000657.
[151] R. Bogue, Smart materials: a review of capabilities and applications, Assem. Autom. 34 (2014) 16–22, doi:10.1108/AA-10-2013-094.
[152] F Momeni, S M.Mehdi Hassani.N, X Liu, J. Ni, A review of 4D printing, Mater. Des. 122 (2017) 42–79, doi:10.1016/j.matdes.2017.02.068.
[153] S Kalia, A Dufresne, BM Cherian, BS Kaith, L Avérous, J Njuguna, et al., Cellulose-Based Bio- and Nanocomposites: a review, Int. J. Polym. Sci. 2011 (2011) 1–35, doi:10.1155/2011/837875.
[154] W Xu, X Wang, N Sandler, S Willför, C. Xu, Three-dimensional printing of wood-derived biopolymers: a review focused on biomedical applications, ACS Sustain. Chem. Eng. 6 (2018) 5663–5680, doi:10.1021/acssuschemeng.7b03924.
[155] L Jiang, X Peng, D. Walczyk, 3D printing of biofiber-reinforced composites and their mechanical properties: a review, Rapid Prototyp. J. 26 (2020) 1113–1129, doi:10.1108/RPJ-08-2019-0214.
[156] ASM Sayem, H Shahariar, J. Haider, An overview on the opportunities for 3D printing with biobased materials, Encycl. Renew. Sustain. Mater. 2 (2020) 839–847, doi:10.1016/b978-0-12-803581-8.10942-7.
[157] D Mohan, ZK Teong, AN Bakir, MS Sajab, H. Kaco, Extending cellulose-based polymers application in additive manufacturing technology: a review of recent approaches, Polymers (Basel) 12 (2020), doi:10.3390/POLYM12091876.
[158] V Klar, J Pere, T Turpeinen, P Kärki, H Orelma, P. Kuosmanen, Shape fidelity and structure of 3D printed high consistency nanocellulose, Sci. Rep. 9 (2019) 3822, doi:10.1038/s41598-019-40469-x.
[159] MA Hubbe, P Tayeb, M Joyce, P Tyagi, M Kehoe, K Dimic-Misic, et al., Nanocellulose rheology, BioResources 12 (2017) 9556–9661.
[160] X Feng, Z Yang, S Chmely, Q Wang, S Wang, Y. Xie, Lignin-coated cellulose nanocrystal filled methacrylate composites prepared via 3D stereolithography printing: mechanical reinforcement and thermal stabilization, Carbohydr. Polym. 169 (2017) 272–281, doi:10.1016/j.carbpol.2017.04.001.
[161] VCF Li, X Kuang, A Mulyadi, CM Hamel, Y Deng, HJ. Qi, 3D printed cellulose nanocrystal composites through digital light processing, Cellulose 26 (2019) 3973–3985, doi:10.1007/s10570-019-02353-9.
[162] Y Chu, Y Sun, W Wu, H. Xiao, Dispersion properties of nanocellulose: a review, Carbohydr. Polym. 250 (2020) 116892, doi:10.1016/j.carbpol.2020.116892.
[163] C Castro, R Zuluaga, C Álvarez, J-L Putaux, G Caro, OJ Rojas, et al., Bacterial cellulose produced by a new acid-resistant strain of gluconacetobacter genus, Carbohydr. Polym. 89 (2012) 1033–1037, doi:10.1016/j.carbpol.2012.03.045.
[164] L Chen, Q Wang, K Hirth, C Baez, UP Agarwal, JY. Zhu, Tailoring the yield and characteristics of wood cellulose nanocrystals (CNC) using concentrated acid hydrolysis, Cellulose 22 (2015) 1753–1762, doi:10.1007/s10570-015-0615-1.
[165] J George, KV Ramana, AS Bawa, Siddaramaiah, Bacterial cellulose nanocrystals exhibiting high thermal stability and their polymer nanocomposites, Int. J. Biol. Macromol. 48 (2011) 50–57, doi:10.1016/j.ijbiomac.2010.09.013.
[166] F Hoeng, A Denneulin, C Neuman, J. Bras, Charge density modification of carboxylated cellulose nanocrystals for stable silver nanoparticles suspension preparation, J. Nanoparticle Res. 17 (2015) 244, doi:10.1007/s11051-015-3044-z.
[167] FM Pelissari, PJ do A Sobral, FC. Menegalli, Isolation and characterization of cellulose nanofibers from banana peels, Cellulose 21 (2014) 417–432, doi:10.1007/s10570-013-0138-6.
[168] IA Sacui, RC Nieuwendaal, DJ Burnett, SJ Stranick, M Jorfi, C Weder, et al., Comparison of the properties of cellulose nanocrystals and cellulose nanofibrils isolated from bacteria, tunicate, and wood processed using acid, enzymatic, mechanical, and oxidative methods, ACS Appl. Mater. Interfaces 6 (2014) 6127–6138, doi:10.1021/am500359f.
[169] S Wickramasinghe, T Do, P. Tran, FDM-based 3D printing of polymer and associated composite: a review on mechanical properties, defects and treatments, Polymers (Basel) 12 (2020) 1529, doi:10.3390/polym12071529.
[170] SV. Murphy, A. Atala, 3D bioprinting of tissues and organs, Nat Biotechnol 32 (2014) 773–785, doi:10.1038/nbt.2958.
[171] A Ji, S Zhang, S Bhagia, CG Yoo, AJ. Ragauskas, 3D printing of biomass-derived composites: application and characterization approaches, RSC Adv. 10 (2020) 21698–21723, doi:10.1039/d0ra03620j.
[172] V Mazzanti, L Malagutti, F. Mollica, FDM 3D printing of polymers containing natural fillers: A review of their mechanical properties, Polymers (Basel) 11 (2019), doi:10.3390/polym11071094.
[173] A Le Duigou, M Castro, R Bevan, N. Martin, 3D printing of wood fibre biocomposites: From mechanical to actuation functionality, Mater. Des. 96 (2016) 106–114, doi:10.1016/j.matdes.2016.02.018.
[174] ME Lamm, L Wang, V Kishore, H Tekinalp, V Kunc, J Wang, et al., Material extrusion additive manufacturing of wood and lignocellulosic filled composites, Polymers (Basel) 12 (2020) 2115, doi:10.3390/polym12092115.
[175] D Stoof, K. Pickering, Sustainable composite fused deposition modelling filament using recycled pre-consumer polypropylene, Compos. Part B Eng. 135 (2018) 110–118, doi:10.1016/j.compositesb.2017.10.005.
[176] Senvol LLC. Senvol 3D Printing Materials Database n.d. http://senvol.com/machine-search/.
[177] A Thumm, D Even, PY Gini, M. Sorieul, Processing and properties of MDF fibre-reinforced biopolyesters with chain extender additives, Int. J. Polym. Sci. 2018 (2018), doi:10.1155/2018/9601753.
[178] A Giubilini, G Siqueira, FJ Clemens, C Sciancalepore, M Messori, G Nystrom, et al., 3D printing nanocellulose-poly(3-hydroxybutyrate-co-3-hydroxyhexanoate) biodegradable composites by fused deposition modeling, ACS Sustain. Chem. Eng. (2020), doi:10.1021/acssuschemeng.0c03385.
[179] Q Wang, C Ji, L Sun, J Sun, J. Liu, Cellulose nanofibrils filled poly(lactic acid) biocomposite filament for FDM 3D printing, Molecules 25 (2020), doi:10.3390/molecules25102319.
[180] HL Tekinalp, X Meng, Y Lu, V Kunc, LJ Love, WH Peter, et al., High modulus biocomposites via additive manufacturing: cellulose nanofibril networks as “microsponges, Compos. Part B Eng. 173 (2019) 106817, doi:10.1016/j.compositesb.2019.05.028.
[181] J Dong, M Li, L Zhou, S Lee, C Mei, X Xu, et al., The influence of grafted cellulose nanofibers and postextrusion annealing treatment on selected properties of poly(lactic acid) filaments for 3D printing, J. Polym. Sci. Part B Polym. Phys. 55 (2017) 847–855, doi:10.1002/polb.24333.
[182] D Filgueira, S Holmen, JK Melbø, D Moldes, AT Echtermeyer, G. Chinga-Carrasco, Enzymatic-assisted modification of thermomechanical pulp fibers to improve the interfacial adhesion with poly(lactic acid) for 3D printing, ACS Sustain. Chem. Eng. 5 (2017) 9338–9346, doi:10.1021/acssuschemeng.7b02351.
[183] L Li, Y Chen, T Yu, N Wang, C Wang, H. Wang, Preparation of polylactic acid/TEMPO-oxidized bacterial cellulose nanocomposites for 3D printing via Pickering emulsion approach, Compos. Commun. 16 (2019) 162–167, doi:10.1016/j.coco.2019.10.004.
[184] A Isogai, T Saito, H. Fukuzumi, TEMPO-oxidized cellulose nanofibers, Nanoscale 3 (2011) 71–85, doi:10.1039/c0nr00583e.
[185] P Siqueira, É Siqueira, AE de Lima, G Siqueira, AD Pinzón-Garcia, AP Lopes, et al., Three-dimensional stable alginate-nanocellulose gels for biomedical applications: Towards tunable mechanical properties and cell growing, Nanomaterials 9 (2019) 1–22, doi:10.3390/nano9010078.
[186] D Rigotti, A Dorigato, A Cataldi, L Fambri, A. Pegoretti, Nanocellulose as reinforcing agent for biodegradable polymers in 3D printing fused deposition modeling, in: ECCM 2018 - 18th Eur. Conf. Compos. Mater., 2020, pp. 24–28.
[187] CA Murphy, MN. Collins, Microcrystalline cellulose reinforced polylactic acid biocomposite filaments for 3D printing, Polym. Compos. 39 (2018) 1311–1320, doi:10.1002/pc.24069.
[188] T Ambone, A Torris, K. Shanmuganathan, Enhancing the mechanical properties of 3D printed polylactic acid using nanocellulose, Polym. Eng. Sci. (2020) 1842–1855, doi:10.1002/pen.25421.
[189] Q Wang, C Ji, J Sun, Q Yao, J Liu, RMY Saeed, et al., Kinetic thermal behavior of nanocellulose filled polylactic acid filament for fused filament fabrication 3D printing, J Appl Polym Sci 137 (2020) 1–9, doi:10.1002/app.48374.
[190] G Melilli, I Carmagnola, C Tonda-Turo, F Pirri, G Ciardelli, M Sangermano, et al., DLP 3D printing meets lignocellulosic biopolymers: carboxymethyl cellulose inks for 3D biocompatible hydrogels, Polymers (Basel) 12 (2020) 1655, doi:10.3390/polym12081655.
[191] G Siqueira, D Kokkinis, R Libanori, MK Hausmann, AS Gladman, A Neels, et al., Cellulose nanocrystal inks for 3D printing of textured cellular architectures, Adv Funct Mater 27 (2017), doi:10.1002/adfm.201604619.
[192] VCF Li, CK Dunn, Z Zhang, Y Deng, HJ. Qi, Direct ink write (DIW) 3D printed cellulose nanocrystal aerogel structures, Sci Rep 7 (2017), doi:10.1038/s41598-017-07771-y.
[193] C Jia, H Bian, T Gao, F Jiang, IM Kierzewski, Y Wang, et al., Thermally stable cellulose nanocrystals toward high-performance 2D and 3D nanostructures, ACS Appl. Mater. Interfaces 9 (2017) 28922–28929, doi:10.1021/acsami.7b08760.
[194] D Nguyen, DA Hgg, A Forsman, J Ekholm, P Nimkingratana, C Brantsing, et al., Cartilage Tissue Engineering by the 3D Bioprinting of iPS Cells in a Nanocellulose/Alginate Bioink, Sci. Rep. 7 (2017) 1–10, doi:10.1038/s41598-017-00690-y.
[195] S Shin, S Park, M Park, E Jeong, K Na, HJ Youn, et al., Cellulose nanofibers for the enhancement of printability of low viscosity gelatin derivatives, BioResources 12 (2017) 2941–2954, doi:10.15376/biores.12.2.2941-2954.
[196] Y Jiang, X Xv, D Liu, Z Yang, Q Zhang, H Shi, et al., Preparation of cellulose nanofiber-reinforced gelatin hydrogel and optimization for 3D printing applications, BioResources 13 (2019) 5909–5924, doi:10.15376/biores.13.3.5909-5924.
[197] MK Hausmann, G Siqueira, R Libanori, D Kokkinis, A Neels, T Zimmermann, et al., Complex-shaped cellulose composites made by wet densification of 3D printed scaffolds, Adv. Funct. Mater. 30 (2020) 1904127, doi:10.1002/adfm.201904127.
[198] LAE Müller, T Zimmermann, G Nyström, I Burgert, G. Siqueira, Mechanical properties tailoring of 3D printed photoresponsive nanocellulose composites, Adv. Funct. Mater. 2002914 (2020) 2002914, doi:10.1002/adfm.202002914.
[199] VCF Li, X Kuang, CM Hamel, D Roach, Y Deng, HJ. Qi, Cellulose nanocrystals support material for 3D printing complexly shaped structures via

multi-materials-multi-methods printing, Addit. Manuf. 28 (2019) 14–22, doi:10.1016/j.addma.2019.04.013.
[200] G Chinga-Carrasco, NV. Ehman, D Filgueira, J Johansson, ME Vallejos, FE Felissia, et al., Bagasse—A major agro-industrial residue as potential resource for nanocellulose inks for 3D printing of wound dressing devices, Addit. Manuf. 28 (2019) 267–274, doi:10.1016/j.addma.2019.05.014.
[201] K Markstedt, A Mantas, I Tournier, H Martínez Ávila, D Hägg, P Gatenholm, 3D bioprinting human chondrocytes with nanocellulose-alginate bioink for cartilage tissue engineering applications, Biomacromolecules 16 (2015) 1489–1496, doi:10.1021/acs.biomac.5b00188.
[202] R Ajdary, NZ Ezazi, A Correia, M Kemell, S Huan, HJ Ruskoaho, et al., Multifunctional 3D-printed patches for long-term drug release therapies after myocardial infarction, Adv. Funct. Mater. 2003440 (2020) 1–10, doi:10.1002/adfm.202003440.
[203] AP Mathew, K Oksman, Z Karim, P Liu, SA Khan, N. Naseri, Process scale up and characterization of wood cellulose nanocrystals hydrolysed using bioethanol pilot plant, Ind. Crops Prod. 58 (2014) 212–219, doi:10.1016/j.indcrop.2014.04.035.
[204] P Gatenholm, H Martinez, E Karabulut, M Amoroso, L Kölby, K Markstedt, et al., Development of Nanocellulose-Based Bioinks for 3D Bioprinting of Soft Tissue, Springer International Publishing, Cham, 2016, doi:10.1007/978-3-319-40498-1.
[205] N Paxton, W Smolan, T Böck, F Melchels, J Groll, T. Jungst, Proposal to assess printability of bioinks for extrusion-based bioprinting and evaluation of rheological properties governing bioprintability, Biofabrication 9 (2017), doi:10.1088/1758-5090/aa8dd8.
[206] MA Hubbe, OJ. Rojas, Colloidal stability and aggregation of Lignocellulosic materials in aqueous suspension: a review, BioResources 3 (2008) 1419–1491, doi:10.15376/biores.3.4.1419-1491.
[207] KMO Hakansson, F Lundell, L Prahl-Wittberg, LD. Söderberg, Nanofibril alignment in flow focusing: measurements and calculations, J. Phys. Chem. B 120 (2016) 6674–6686, doi:10.1021/acs.jpcb.6b02972.
[208] KMO Håkansson, AB Fall, F Lundell, S Yu, C Krywka, SV. Roth, et al., Hydrodynamic alignment and assembly of nanofibrils resulting in strong cellulose filaments, Nat. Commun. 5 (2014), doi:10.1038/ncomms5018.
[209] MK Hausmann, PA Rühs, G Siqueira, J Läuger, R Libanori, T Zimmermann, et al., Dynamics of cellulose nanocrystal alignment during 3D printing, ACS Nano 12 (2018) 6926–6937, doi:10.1021/acsnano.8b02366.
[210] N Yoshiharu, K Shigenori, W Masahisa, O. Takeshi, Cellulose microcrystal film of high uniaxial orientation, Macromolecules 30 (1997) 6395–6397, doi:10.1021/ma970503y.
[211] A. Dufresne, 1. Cellulose and potential reinforcement, in: Nanocellulose, De Gruyter, Berlin, Boston, 2017, pp. 1–46, doi:10.1515/9783110480412-002.
[212] KMO. Håkansson, Online determination of anisotropy during cellulose nanofibril assembly in a flow focusing device, RSC Adv. 5 (2015) 18601–18608, doi:10.1039/C4RA12285B.
[213] K Markstedt, J Sundberg, P. Gatenholm, 3D bioprinting of cellulose structures from an ionic liquid, 3D Print Addit. Manuf. 1 (2014) 115–121, doi:10.1089/3dp.2014.0004.
[214] DHAT Gunasekera, S Kuek, D Hasanaj, Y He, C Tuck, AK Croft, et al., Three dimensional ink-jet printing of biomaterials using ionic liquids and co-solvents, Faraday Discuss 190 (2016) 509–523, doi:10.1039/c5fd00219b.
[215] L Li, Y Zhu, J. Yang, 3D bioprinting of cellulose with controlled porous structures from NMMO, Mater. Lett. 210 (2018) 136–138, doi:10.1016/j.matlet.2017.09.015.
[216] SW Pattinson, AJ. Hart, Additive manufacturing of cellulosic materials with robust mechanics and antimicrobial functionality, Adv. Mater. Technol. 2 (2017) 1600084, doi:10.1002/admt.201600084.
[217] TM Tenhunen, O Moslemian, K Kammiovirta, A Harlin, P Kääriäinen, M Österberg, et al., Surface tailoring and design-driven prototyping of fabrics with 3D-printing: an all-cellulose approach, Mater. Des. 140 (2018) 409–419, doi:10.1016/j.matdes.2017.12.012.
[218] R Hu, B Huang, Z Xue, Q Li, T Xia, W Zhang, et al., Synthesis of photocurable cellulose acetate butyrate resin for continuous liquid interface production of three-dimensional objects with excellent mechanical and chemical-resistant properties, Carbohydr Polym. 207 (2019) 609–618, doi:10.1016/j.carbpol.2018.12.026.
[219] Mostakim K, Shahriar F, Arefin A, Rafi H. Polymer as smart material for 4D printing: A review 2019;2019:11–3.
[220] YS Zhang, K Yue, J Aleman, K Mollazadeh-Moghaddam, SM Bakht, J Yang, et al., 3D bioprinting for tissue and organ fabrication, Ann. Biomed. Eng. 45 (2017) 148–163, doi:10.1007/s10439-016-1612-8.
[221] A Sydney Gladman, EA Matsumoto, RG Nuzzo, L Mahadevan, JA. Lewis, Biomimetic 4D printing- supporting information, Nat. Mater. 15 (2016) 413–418, doi:10.1038/nmat4544.
[222] S Poppinga, D Correa, B Bruchmann, A Menges, T. Speck, Plant movements as concept generators for the development of biomimetic compliant mechanisms, Integr. Comp. Biol. 60 (2020) 886–895, doi:10.1093/icb/icaa028.
[223] S Sultan, HN Abdelhamid, X Zou, AP. Mathew, CelloMOF: nanocellulose enabled 3D printing of metal–organic frameworks, Adv. Funct. Mater. 29 (2019) 1–12, doi:10.1002/adfm.201805372.